ELSEVIER

Coordination Chemistry Reviews 142 (1995) 43–99

COORDINATION CHEMISTRY REVIEWS

3. Iron 1992

Ebbe Nordlander and Anne M. Whalen

CONTENTS

SSDI 0010-8545 (94) 05001-5

INTRODUCTION

This review covers the coordination chemistry of iron for 1992. The following journals have been covered by a combination of searching in *Chemical Abstracts* and independent searches in the following journals: *Acta Chemica Scandinavica*; *Acta Crystallographica, Sect. C*; *Angewandte Chemie International Edition in English*; *Bulletin of the Chemical Society of Japan*; *Bulletin de la Société Chimique de France*; *Chemische Berichte*; *Chemistry Letters*; *Chemistry Reviews*; *Coordination Chemistry Reviews*; *Gazzetta Chimica Italiana*; *Helvetica Chimica Acta*; *Indian Journal of Chemistry, Section A*; *Inorganic Chemistry*; *Inorganica Chimica Acta*; *Journal of the American Chemical Society*; *Journal of the Chemical Society, Chemical Communications*; *Journal of the Chemical Society, Dalton Transactions*; *Journal of Coordination Chemistry*; *Journal of the Indian Chemical Society*; *Mendeleev Communications*; *New Journal of Chemistry*; *Polyhedron*; *Recueil des Travaux Chimiques de Pays-Bas*; *Transition Metal Chemistry (London)*; *Zeitschrift für Anorganische und Allgemeine Chemie*; *Zeitschrift für Naturforschung*.

Although carbonyl compounds have been included in the previous iron reviews in this journal, they have, for the purpose of this review, been classified as organometallic compounds and are not included. Most iron-heterometal complexes have been excluded. All reported magnetic exchange values have been normalized to fit the following exchange Hamiltonian: $H = -2J\ S_1 \cdot S_2$. This review does not aim to be fully comprehensive; omissions or errors are entirely the fault of the authors.

3.1 COMPLEXES WITH HYDROGEN OR HYDRIDE LIGANDS

The complexes $FeH_3(PPh_2R')_3ER_3$ (R' = n-Bu (ER_3 = $SnPh_3$, $SiMePh_2$); R' = Et (ER_3 = $SnPh_3$)) were prepared by reaction of $Fe(H)_2(H_2)(PPh_2R')_3$ with $HSnPh_3$ or $HSiMePh_2$ [1]. The crystal structure of $FeH_3(PPh_2Et)_3SnPh_3$ shows an approximate C_3 symmetry in the molecule and a nearly tetrahedral FeP_3Sn core. Variable temperature ^1H and ^{31}P NMR spectra suggest that at low temperatures the complexes are (pseudo-)octahedral with three facial phosphine ligands, two terminal hydrides and an η^2-coordinated H-ER_3 ligand (an Fe, H, Si(Sn) three-centre two-electron bond).

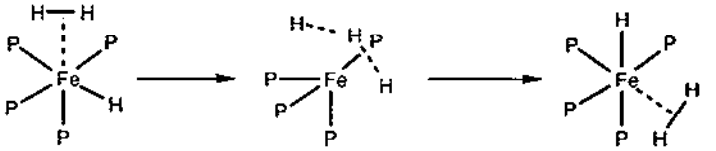

Scheme 1: *A possible mechanism for intramolecular hydrogen/hydride exchange in cis-$[Fe(PR_3)_4H(H_2)]^+$ complexes.*

Several possible mechanisms for intramolecular atom exchange between molecular hydrogen and hydride ligands in *cis*-$[Fe(PR_3)_4H(H_2)]^+$ complexes has been studied in an *ab initio* theoretical study. The favoured mechanism is a single step transfer ("open direct transfer") of the hydrogen

atom between the two ligands. In the transition state of this mechanism the central hydrogen atom is bound to the other two hydrogens (Scheme 1) [2].

3.2 COMPLEXES WITH HALIDE LIGANDS

The cation FeF^+ has been generated in a Fourier transform ion-cyclotron-resonance mass spectrometer *via* C-F bond activation by reacting bare FeO^+ with hexafluorobenzene [3]. Bracketing experiments provide a bond dissociation energy (BDE) for FeF^+ of 86 < BDE< 101 kcal mol^{-1} which may be compared to the BDE value of 100.9 kcal mol^{-1} predicted from CAS-MCSCF psuedopotential *ab initio* calculations. In another mass spectrometry experiment, the electron affinity of $FeCl_3$ has been determined to be 417±17kJ mol^{-1} by determination of $FeCl_2$ with $[Al_xCl_{4-x}]^-$ (x = 0-2) in the gaseous phase through Knudsen cell mass spectrometry; this is approximately 1 eV higher than the electron affinity for FeF_3 [4].

Iron trichloride or its hexahydrate has been used for the catalytic oxidation of hydrocarbons. Murahashi *et al.* [5] have investigated the catalytic oxidation of alkanes and alkylated arenes using iron powder, $Fe(OAc)_3$ or $FeCl_3 \cdot 6\ H_2O$ as catalysts. Reaction of tertiary carbons with molecular dioxygen (1 atm) at room temperature in the presence of catalytic amounts of acetic acid and iron powder/complex yields alcohols; the reaction of secondary carbons under similar conditions affords ketones. Aldehydes used include acetaldehyde, 2-methylpropanal and heptanal, the latter being the most efficient. Acids used were, in order of decreasing efficiency: acetic acid, chloroacetic acid and trifluoroacetic acid.

Similarly, Shul'pin *et al.* [6] have used $FeCl_3$ to catalyse the hydroxylation of alkanes. Irradiation of cyclohexane, pentane, hexane and heptane in various alcohols in the presence of $FeCl_3 \cdot 6\ H_2O$ yields alcohols as the major product(s) with some formation of ketones. The reactivity of the C-3 C-H bond in hexane is enhanced in comparison to C-2 and C-1; similarly, the C-4 C-H bond is the most reactive in heptane. The reaction is proposed to be initiated by chlorine radicals formed by homolysis of the Fe-Cl bonds.

3.3 COMPLEXES WITH CYANIDE LIGANDS

The kinetics of replacement of 4-cyanopyridine (4-CNpy) by CN^- in $[Fe(CN)_5(4\text{-}CNpy)]^{3-}$ have been studied in aqueous $NaNO_3$, $LiNO_3$, NaCl and $NaClO_4$ solutions. The reaction is believed to proceed *via* a limiting dissociative (D) mechanism. The salt effects on the reactivity of this system were found to be minor [7].

The dimeric complex $[Fe_2(CN)_{10}]^{4-}$ is reduced to the mixed-valence species $[Fe_2(CN)_{10}]^{5-}$ by the iodide ion. The reaction mechanism is believed to involve the formation of I^{2-} as a reaction intermediate [8]. The equilibrium constants and reaction rates are strongly dependent on the nature of the cation, indicating that complexation/ion-pairing with the cations takes place. Reduction is favoured in the sequence $Cs^+ > NH_4^+ \gg K^+ > Na^+ > Li^+$.

The reaction of $[FeH(\mu_2\text{-}H_2)\{P(OEt)_2Ph\}_4]^+$ with $NOPF_6$ yields $[FeH(NO)\{P(OEt)_2Ph\}_4]^+$ (**1**). The resultant nitrosyl complexes may be reacted with an excess of

isocyanide to form $[FeH(NO)(CNR)_2\{P(OEt)_2Ph\}_4]^+$. The NMR and IR spectra of the latter complex indicate that the two isocyanide ligands are *cis*-coordinated [9].

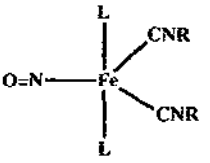

(1)

3.4 COMPLEXES WITH NITROGEN DONOR LIGANDS

3.4.1 Complexes with N-heterocyclic ligands

3.4.1.1 Complexes with pyridine and polypyridine ligands

The reaction of $Fe(NCS)_2$ with *trans*-4-styrylpyridine (t-stpy) yields $[Fe(t\text{-}stpy)_2(MeOH)_2(NCS)_2)_2(t\text{-}stpy)]$, an iron(II) spin cross-over species containing a photoisomerizable ligand. Magnetic susceptiblility measurements showed that the metal ion is in the high spin state from 300 to 4 K, which is similar to the results for $[Fe(py)_4(NCS)_2]$. The two uncoordinated t-stpy molecules lie nearly parallel to the coordinated ones and are strongly hydrogen bonded to the MeOH ligands, probably through one of the C-H groups of the phenyl ring [10].

The crystal structure of tris(4-fluoro-2,2'-bipyridyl)iron(II) hexafluorophosphate (2) has been determined. The structure is disordered with respect to the location of the fluorine atoms. Site occupancy was refined so as to achieve a 3:1 (*mer* :*fac*) ratio which is in accordance with ^{19}F NMR spectroscopic studies [11].

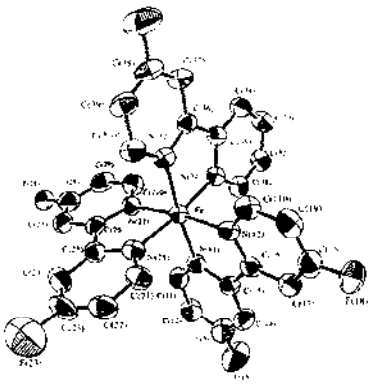

Crystal structure of (2).

The reaction of pyterpy (pyterpy = 4'-(4'''-pyridyl)-2,2':6',2''-terpyridine, (3)) with $[Fe(H_2O)_6)]^{2+}$ results in the formation of $[Fe(pyterpy)_2]^{2+}$ in which each pyterpy ligand is

tridentate; the 4-pyridyl rings do not coordinate [12]. The pyterpy complex exhibits a reversible Fe(II/III) oxidation process at slightly more positive ($\Delta E_{1/2}$ = 30 mV) potential and a longer wavelength MLCT band than the analogous terpy complex (2,2':6',2"-terpyridine) in accordance with pyterpy being a better π-acceptor than terpy. The complex may be protonated or methylated at the free 4-pyridyl groups.

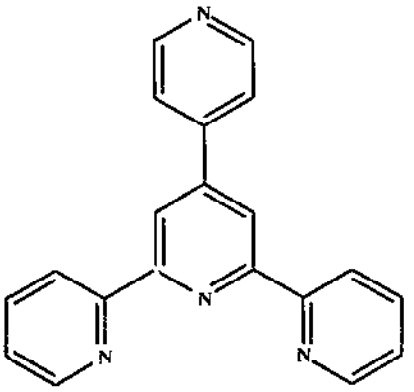

(3)

The ligand (4) which consists of two 2,2',6',2"-terpyridine chelates connected by a $-CH_2CH_2-$ linker *via* two positions *meta* to the pyridine nitrogen atoms specifically forms double stranded helical complexes with divalent metal ions. The Fe(II) complex of this ligand has been characterized by fast atom bombardment mass spectrometry and ^1H NMR spectroscopy [13].

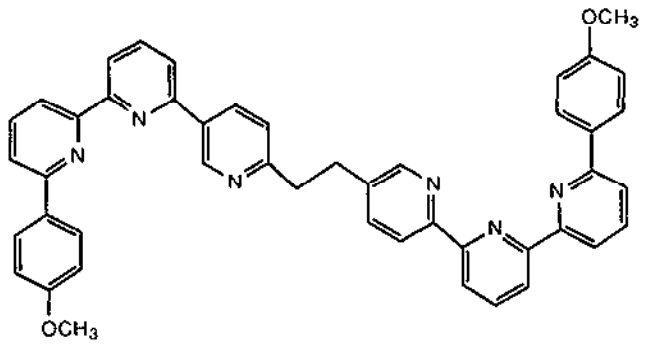

(4)

3.4.1.2 Complexes with other N-heterocyclic ligands

A new route to the anionic complex $[(HBpz_3)FeCl_3]^-$ has been devised. The complex is obtained from the reaction of $FeCl_3 \cdot 6\ H_2O$ with $KHBpz_3$ in methanol followed by addition of $(Et_4N)Cl$ to form the ammonium salt [14].

The synthesis and properties of an iron complex [FeCl(TIM)]Cl of the tetraimidazole ligand bis((imidazol-4'-methyl)-4-imidazol-2-yl) methane (TIM), (5), has been reported by Mulliez *et al.* [15]. In the solid state, the high spin iron(II) is pentacoordinated with a distorted trigonal bipyramid. In methanol solution, the coordinated chloride is displaced and the complex becomes hexacoordinated with solvent molecules as auxiliary ligands. The iron redox potential of this complex together with the EPR spectroscopic characteristics of the ferric form present a relevant model for the iron binding site of the soybean lipooxygenases.

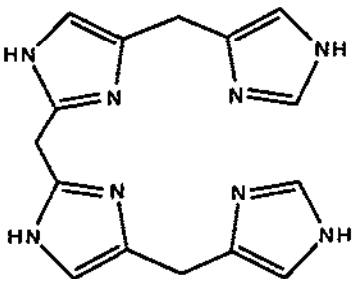

(5)

Ferrous complexes of haph (*N*-(2-imidazol-3-ylethyl)-6-[(2-imidazolylethylamino)methyl]-pyridine-2-carboxamide, (6) have been promoted as bleomycin analogues [16]. It has been found that Fe(II)(haph)-O_2 exhibits approximately one tenth of the Bleomycin activity for DNA cleavage. Cleavage of a 111-bp DNA plasmid has been effected both by Fe(II)haph-O_2 and Fe(III)haph-H_2O_2. Nicking of DNA by Fe(II)(haph) is not suppressed by the addition of the hydroxyl radical scavenger DMSO, a result which is seen to indicate that the dominant mechanism for DNA cleavage by this complex is not due to generation of free hydroxyl radicals. It is proposed that the ferrous complex generates an active ferryl species *via* hydroxyl abstraction from an Fe(III)(haph)hydroperoxo intermediate.

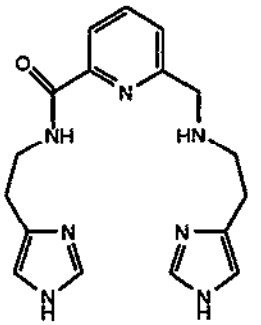

(6)

3.4.2 Complexes with imines and oximes

Reaction of the semicorrin (7) with $FeSO_4$ gives the distorted tetrahedral chelate bis{(1S, 9S)-5-cyan-1,9-bis(methoxycarbonyl)semicorrinato)}Fe(II), the crystal structure of which has been determined. The EPR and Mössbauer spectra are consistent with the crystal structure; the isomer shift of the Mössbauer spectrum (δ = 0.93 mm s^{-1} at 4 K) is typical for a tetrahedral Fe(II) ion [17].

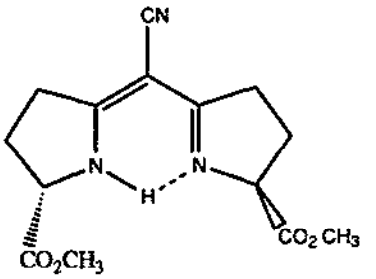

(7)

The complex $[FeL_2] \cdot 2$ dme (8), (L = 1,2,6,7-tetracyano- 3,5-dihydro-3,5-diimino-pyrrolizinide) has been prepared and its crystal structure has been determined [18]. The central metal atom, which lies on a symmetry centre, coordinates four imino groups in a square-planar arrangement within the ligand equatorial plane, and completes its octahedral, tetragonally distorted $MNeq_4Nax_2$ coordination geometry with two axial cyano groups from two crystallographically equivalent complex molecules. Variable-temperature magnetic measurements show that the complex is a high-spin (S = 2) Fe(II) species with antiferromagnetic superexchange interactions. The optical spectrum is very similar to that of corresponding metal phthalocyanine complex. The complex can be chemically oxidized by O_2 in MeCN solution to give insoluble polymeric species, corresponding analytically to $[FeL_3(O_2)] \cdot 6$ MeCN. This complex is a superoxo adduct in which the dioxygen is centrosymmetrically bridged between the metal atoms in the formal oxidation state Fe(IV) and Fe(III).

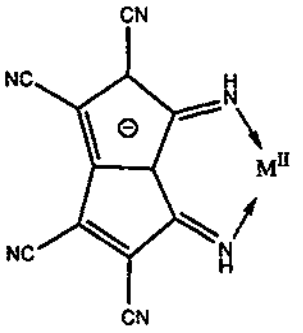

(8)

3.4.3 Complexes with macrocyclic ligands

The complex $[Fe(HL)NO]NO_3$ (**9**) (H_3L = 2,4-pentanedione bis(*S*- methylisothiosemicarbazone)) has been prepared by the template reaction of *S*-methylisothiosemicarbazidehydrogen nitrate, Na(acac) · H_2O, and $Fe(NO_3)_3 \cdot 9H_2O$ in EtOH, while $[Fe(R_2Q)NO]$ (R = Me (**10**), Et (**11**), Pr (**12**), Bu (**13**)) was obtained by the interaction of $Fe(NO_3)_3 \cdot 9H_2O$ with nitromalondi-aldehyde bis(*S*-methylisothiosemicarbazone) (R_3H_3Q) in the presence of NO in EtOH [19]. Complexes (**9**) and (**12**) have square-pyramidal structures, with the corresponding quadridentate ligand (HL^{2-} and PrQ^{3-}) around the central ion in the basal plane and the NO in the apical position. The FeNO group is approximately linear. Crystallographic and IR, and Mössbauer spectroscopic data, as well as calculations of the electronic structures indicate that the FeNO group is a highly covalent entity which corresponds to the Fe(III)NO rather than the $Fe(IV)NO^-$ state.

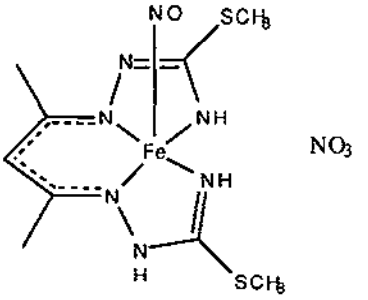

(**9**)

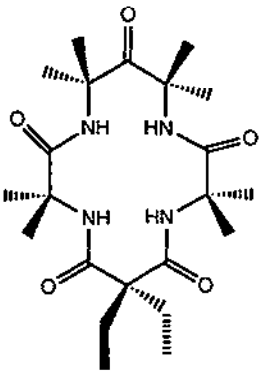

(**14**)

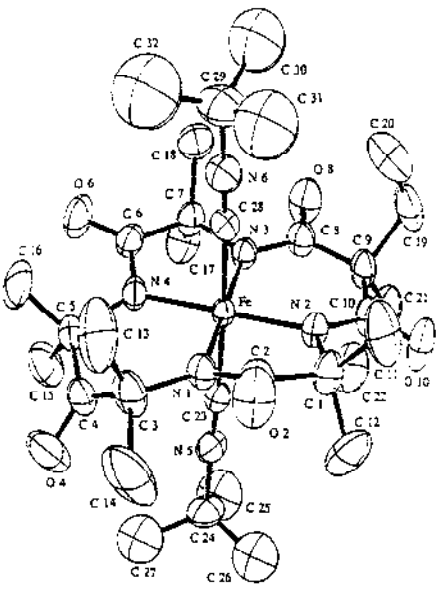

Crystal structure of Fe{η4-(**14**)}$(CNBut)_2$.

The addition of ^{t}BuNC to the dilithium salt of the chloroiron complex of the tetraaminoligand (**14**) in water followed by addition of $(NH_4)_2Ce(NO_3)_6$ results in the formation of Fe{η4-(**14**)}$(CNBut)_2$, a stable Fe(IV)complex [20]. Cyclic voltammetry in CH_2Cl_2 shows a reversible Fe IV/III couple at approx 1.16 V vs. NHE. The zero-field Mössbauer spectrum is consistent with an S = 1 Fe(IV) centre with a rhombically distorted t_2g^4 configuration.

The reaction of $FeBr_2$ with the 1,4,7,10-tetrakis(pyrazol-1-ylmethyl)-1,4,7,10-tetraazacyclododecane (**15**) in an acetone/ethanol solution yields a mixture of the octacoordinate complex $[FeL]^{2+}$ and the heptacoordinate $[FeL']^{2+}$ (L' = (**16**) = ethoxy derivative of (**15**)) as evidenced by X-ray crystallography [21].

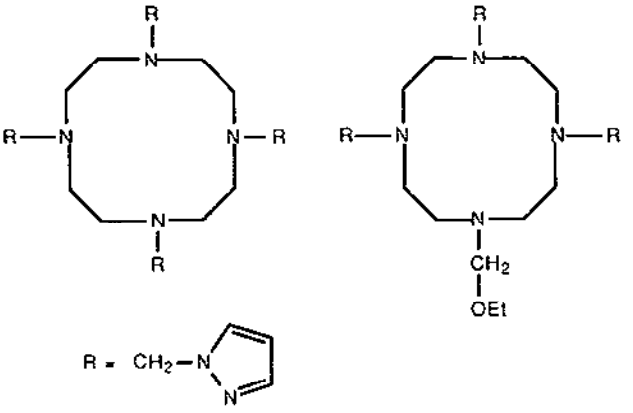

(**15**) (**16**)

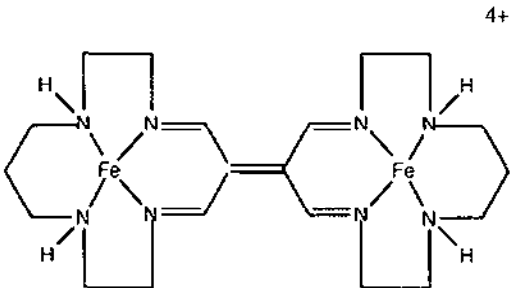

(**17**)

In the diiron complex $[Fe_2(C_{20}H_{36}N_8)(C\text{-}H_3CN)_4](ClO_4)_4 \cdot 2CH_3CN$, (**17**), two fourteen-membered macrocycles containing β-imine nitrogens are linked through a double bond between corresponding bridgehead carbons [22]. The X-ray crystallographic determination establishes the double bond bridge and unusually short iron(II)-nitrogen bond distances. The planar structure of the complex promotes extensive delocalization in the π electron system and the short bonds may be a result of this delocalization. The diiron complex also exhibits an intense low energy absorption band at 874 nm (14000 M^{-1} cm^{-1}) in acetonitrile. This band has been assigned to an MLCT charge

transfer, where an electron from the filled $d_{xy}d_{yz}$ orbitals of Fe is transferred to a low-lying delocalized π^* orbital of the tetraiminoethylene moiety.

3.4.4 Miscellaneous N-donor complexes

The synthesis of $Fe(abpt)_2(tcnq)_2$ (abpt = 3,5-bis(pyridin-2-yl)-4-amino-1,2,4-truazole), (**18**)) has been achieved by the reaction of $Fe(abpt)_2(NO_3)_2$ with Li(TCNQ) in a mixture of acetonitrile and methanol. Conductivity measurements on pressed pellets show that the compound is essentially an insulator [23].

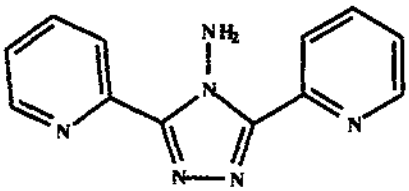

(**18**)

The Mössbauer and electronic spectra of ferrous complexes with the tridentate ligands L of the type 2,6-bis(benz-X-azol-2-yl)pyridine (X- = imid-, thi-, ox-), (**19**), have been determined. For the complexes of type $[FeL_2]^{2+}$, benzimidazole ligands give low-spin complexes, benzoxazoles give high-spin and benzthiazole complexes exhibit spin-crossover properties [24]. The Mössbauer isomer shifts decrease in the order benzoxazole>benzthiazole>benzimidazole. Complexes of the type $FeLX_2$ (X = Cl, ClO_4) are all high spin. A low- to high spin transition which occurs for the compound $[Fe(2,6\text{-benzimidazol-pyridine})_2]^{2+}$ upon warming in dmf solution, is attributed to dissociation of the complex to yield the free (solvated) high-spin Fe(II). The crystal structure of $[Fe(bzimpy)_2](CF_3SO_3)_2 \cdot 2\,EtOH$ has been determined.

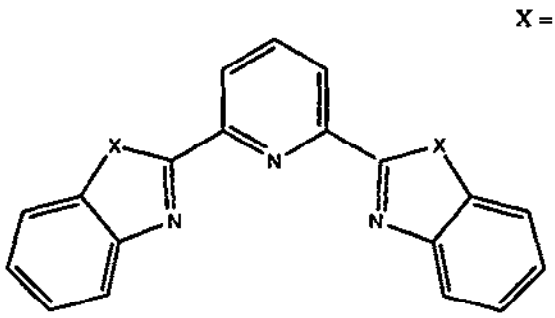

X = NH; bzimpy
NMe; mbzimpy
S; bzthpy
O; bzoxpy

(**19**)

The low-spin complexes $[Fe(bpc)L_2]ClO_4$ (H_2bpc = 4,5-dichloro-1,2-bis(2-pyridinecarboxamidobenzene (**20**); L = Bu_3P, imidazole (Im), 1-MeIm, 4-tert-butylpyridine) and $[Fe(bpc)(H_2O)Cl]$ have been prepared [25]. The complexes display reversible one-electron

oxidation/reduction couples. The stable one-electron-oxidized species $[Fe(bpc)(Bu_3P)_2]^{2+}$ has been generated electrochemically. The UV/VIS spectra of these complexes show broad absorptions in the 740-750 nm region which are assigned as ligand to metal charge transfer transitions.

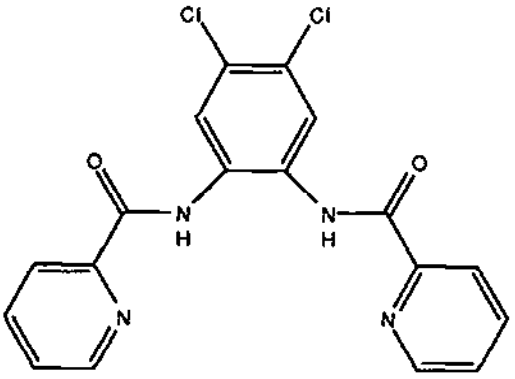

(20)

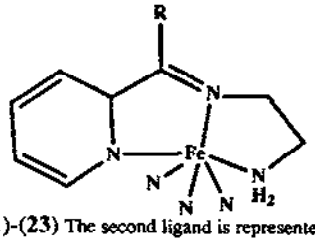

R = H:tsbh
Me:tsbm
Ph:tsbp

(21)-(23) The second ligand is represented by three nitrogen atoms.

The kinetics of base hydrolysis of the related Schiffs base complexes $[Fe(tsbh)_2](ClO_4)_2$ (21), $[Fe(tsbm)_2](ClO_4)_2$ (22) and $[Fe(tsbp)_2](ClO_4)_2$ (23) in H_2O/methanol solutions have been studied [26]. It is suggested that the reactions proceed by nucleophilic attack of the hydroxide ion at the azomethine carbons of the ligands.

The structure of diaquadichlorobis(hydrazinium)iron(II) dichloride (24) has been determined [27].

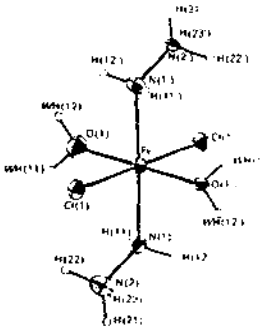

Crystal structure of (24).
Reprinted with permission from [11, 27]. Copyright International Union of Crystallography.

3.5 Complexes with tetrapyrrole macrocycles

3.5.1 Complexes with phthalocyanines

The macrocyclic complex tetracyanonaphthalocyaninatoiron(II) [$(CN)_4$-2,3NcFe] (**25**) is synthesized from the high-temperature reaction of the ligand precursor 2,3,6-tricyanonaphthalene with $Fe(OAc)_2$. Reaction of this complex with the neat ligands ^tBuNC, cyclohexylisocyanide and adamantylisocyanide results in bis-axial coordination to form $(CN)_4$-2,3NcFe$(NCR)_2$ (R = t-butyl, cyclohexyl, adamantyl). The analogous reaction with 1,4-diisocyanobenzene (dib) affords the bridged complex $[QFe(dib)]_n$, which exhibits only poor semiconducting properties when compared to $[Q'Fe(dib)]_n$ (Q' = 2,3-naphthocyanine). The bridged complex may be doped with iodine, and the resulting product $[QFe(dib)I_{1.4}]_n$ shows a powder conductivity, $\sigma_{RT} = 2 \times 10^{-5}$ S cm^{-1}, at room temperature [28].

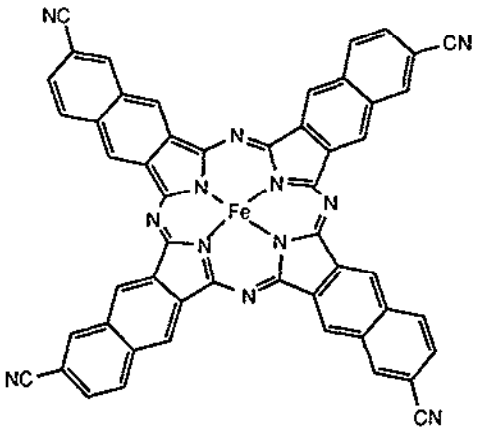

(**25**)

3.5.2 Complexes with porphyrins

3.5.2.1 Axially ligated porphyrin complexes

The synthesis and characterization of $[Fe(TMP)L_2]ClO_4$ (L = 4-amino- (**26**), 3-ethyl- (**27**), 3-chloro- (**28**), 4-cyano-(**29**), 3-cyanopyridine (**30**), 2-methylimidazole (**31**)) are reported [29]. The crystal structures of three of these complexes (**27**)-(**29**) reveal that the axial ligands have a relative perpendicular alignment with bond lengths consistent with low-spin Fe(III). The porphinato cores are strongly S_4 ruffled. Large g_{max} type EPR spectra are observed; the 3-ethyl-, 3-chloropyridine and 2-methylimidazole complexes have unusually low g values (<3.2) rather than g≥3.4 which may be expected for perpendicular ligand orientation. The 4- and 3-cyanopyridine complexes have axial EPR spectra with $g_\perp = 2.53$ and $g_\parallel = 1.56$ or $g_\perp = 2.62$ and $g_\parallel$ unresolved, which result from a substantial change in the usual ground state of low-spin (porphinato)iron(III) complexes, $(d_{xy})^2(d_{xz},d_{yz})^3$, to that having a predominantly $(d_{xz},d_{yz})^4(d_{xy})^1$ ground state. The Mössbauer quadrupole splittings are also unusually low for (porphinato)iron(II) complexes complexes with perpendicular angular imidazole ligand orientation.

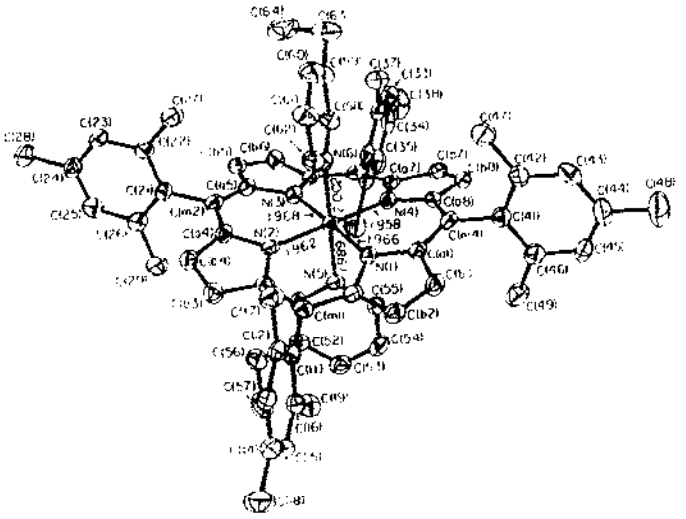

Crystal structure of (27).
Reprinted with permission from [29]. Copyright 1992 American Chemical Society.

Detailed NMR spectroscopic investigations of a large number of mono-*ortho*-substituted derivatives of $[(TPP)Fe(NMeIm)_2)]^+$ have shown that only when the substituent is a C-bound amide, *o*-$CONR_2$, is one axial ligand hindered in its rotation about the Fe-N(Im) bond [30]. Other *ortho* substituents such as -NO_2, -OR, or -NHCOR are either not large enough (-NO_2), or not sterically rigid enough to place the bulky part of the substituent close enough to the axial ligand (-OR, -NHCOR).

The reaction of $[K(18C6)(H_2O)][Fe(NO_2)_2(TPivPP)]$ with an excess of 2,3,5,6-tetrafluorothiophenolate in benzene yields $[K(18C6)(H_2O)][Fe(NO_2)(SC_6HF_4)(TPivPP)]$ (**32**) which has been characterized by UV-VIS, IR, EPR and Mössbauer spectroscopies as well as X-ray diffraction. The latter reveals that the sterically less bulky nitro group is bound on the pocket side of the porphyrin whereas the larger tetrathiophenolate ligand is bound on the open face. On the other hand, the reaction of the same starting material with tetrafluorothiophenol rather than the thiolate, results in the reduction to the corresponding ferrous nitrosyl porphyrin complex and the transfer of one nitro group to the K(18C6) cation [31].

Indirect detection of ^{57}Fe NMR spectroscopic resonances in phosphine-substituted ^{57}Fe-enriched iron-porphyrin complexes has been achieved by observing the $(^{57}Fe)^{31}P$-resonances of the compounds. Measurement of the decoupled ^{31}P-resonances of $[(X)_4TPPFe(PMe_3)_2]$ (X = Cl, OCH_3) and $[(TPP)Fe(PMe_3)(L)]$ (L = CO, ^{n}BuNC, ^{n}BuNH$_2$, $PhCH_2SCH_3$, NMeIm, 4-NMe_2py, py, 4-CNpy) indicates that the ^{57}Fe and ^{31}P shifts are correlated, *i.e.* it appears that the various ligands affect the shielding of the phosphorus and iron nuclei in the same manner [32].

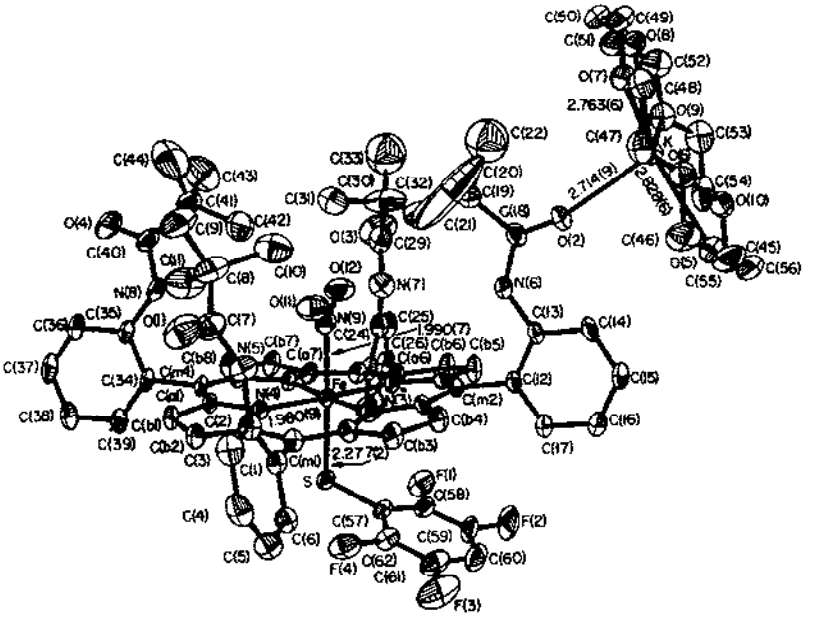

Crystal structure of (32)
Reprinted with permission from [31]. Copyright 1992 American Chemical Society.

Electronic absorption and resonance Raman spectra are reported for complexes of iron(II) tetrakis((*N*-tert-butylcarbamoyl)phenyl)porphyrin, [Fe(II)(T^{t}ButPP)] in wet methylene chloride or toluene [33]. The meso-phenyl groups contain reversed secondary amide groups with respect to those included in the "picket-fence" ferroporphyrin [Fe(II)(TPivPP]. Spectroscopy shows that [Fe(II)(T^{t}ButPP)] can bind a water molecule, forming a five-coordinate high-spin complex. The stabilization of this aquo complex is attributed to the formation of (an) internal H-bond(s) between the coordinated water molecule and one (or two) of the four carbamoyl carbonyl groups of the porphyrin. A comparison of resonance Raman spectra obtained for the [Fe(II)(T^{t}ButPP)(1-MeIm)] and [Fe(II)(T^{t}ButPP)(H_2O)] (33) complexes with available Raman spectroscopic data on deoxymyoglobin suggests that deoxyhemoproteins at low pH could transiently bind a water molecule after rupture of the normal heme-His ligation.

Iron(II)octaethyltetraazaporphyrin [Fe(II)(OETAP)], (34), has been synthesized by the heating of a toluene/thf-solution of OETAP, FeI_2 and 2,6-lutidine [34]. An iron(III) derivative (35) is obtained by the treatment of the ferrous compound with HCl. Magnetic susceptibility data (Faraday method) indicate a spin state of S = 1 for the ferrous compound and S = $^3/_2$ for the ferric compound. Cyclic voltammetry of the six-coordinate bis-py and bis-MeIm derivatives shows that the III/II redox couple is shifted more than 400 mV to positive potentials when compared to the analogous octaethylporphyrin (OEP) complexes.

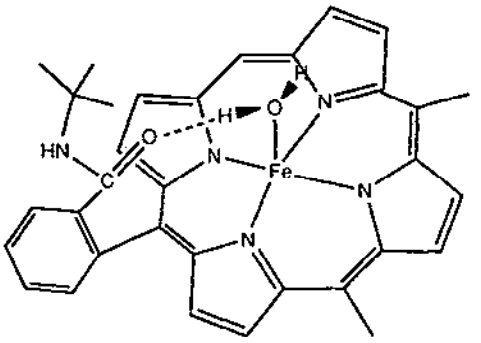

(33)

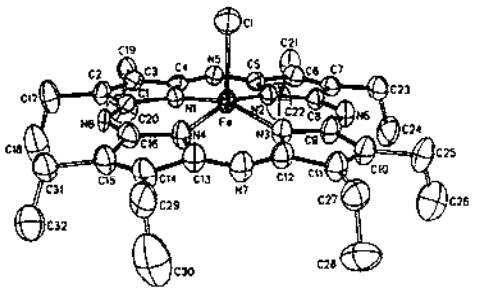

Crystal structure of (35).

The copper complex [Cu(**36**)] and the nickel complex [Ni(**37**)] contain sterically hindered imidazole rings. These complexes have been used as substituted imidazole ligands for Fe(II) and Fe(III) complexes [35]. UV-VIS spectroscopy indicates that the reaction of Cu(**36**) with Fe(TMP)OH results in the formation of the penta-coordinate species [Fe(TMP)·Cu(**36**)]$^{+}OH^{-}$. Completion of the coordination sphere of iron by solvent or hydroxide is possible. The reaction of [Fe(TMP)·Ni(**37**)]ClO_4 to air results in rapid hydrolysis to the corresponding μ-oxo dimer. Variable temperature magnetic moment measurements are consistent with an admixed intermediate-spin complex which is attributed to strong axial distortion.

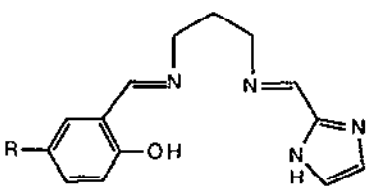

(**36**) R = H; (**37**) R = OMe

It has been shown that when [Fe(III)(TPFPP)Cl] is reacted with azaferrocene in $CHCl_3$, coordination of ferrocene and concomitant reduction takes place, resulting in the formation of $[Fe(TPFPP)(Fe(Cp)(C_4H_4N)]_2$ [36]. The ferrous complex may be reoxidized in an aerated chloroform solution. The low-temperature ESR spectrum indicates that the oxidized species is high-spin iron(III), possibly [Fe(TPFPP)(OH)]. Under the same conditions, azaferrocene does not coordinate to the less easily reduced [Fe(TPP)(Cl)] or [Fe(OEP)Cl]. Neither does the stronger reductant ferrocene reduce [Fe(TPFPP)Cl]. It appears that reduction does only occur upon coordination of azaferrocene (and vice versa).

3.5.2.2 Complexes with oxygen, peroxides and hydroxides

The oxidative action of *m*-chloroperoxybenzoic acid on the triflato complexes of [tetrakis(2,6-dichlorophenyl)porphyrinato]- (TDCPP) and [tetrakis(2,4,6-trimethoxyphenyl)-(TMOP) porphyrinato]-iron(III) generated the corresponding oxoferryl porphyrin π-cation radical complexes $[Fe(IV)=O(TMOP)]^+$ and $[Fe(IV)=O(TDCCP)]^+$ [37]. High frequency resonance Raman spectroscopic data confirm that these complexes are π-cation radicals. The EPR spectra of the complexes indicate ferromagnetic coupling between the ferryl and porphyrin π-cation radical spins yielding quartet states; this is corroborated by Mössbauer data.

A new oxo-perferryl porphyrin complex has been synthesized through oxidation of Fe(TDCPP)*m*-chlorobenzoate with 1.8 equivalents of *p*-nitrobenzoic acid in dry dichloromethane in the presence of *m*-chlorobenzoic acid at –90°C [38]. Addition of four equivalents of methanol causes disappearance of the UV-VIS band due to the ligand radical; the resultant product exhibits an EPR spectrum and is formulated as a ferryl species. The reactivity of both products with respect to the epoxidation of norbornene was investigated; the perferryl was found to be approximately 10 times more reactive than the ferryl species.

An a_{1u} oxoiron(IV) porphyrin π-cation radical $[(TMTMP)Fe(IV)=O]^{+\cdot}$ was synthesized and characterized by hyperfine shifted NMR spectroscopic studies ($TMTMPH_2$ = tetramethyl-3,8,13,18-tetramesitylporphyrin). Large downfield shifted signals were seen for the pyrrole β-methyl- and the meso protons. The calculated π-spin densities at the pyrrole β and *meso* carbon atoms of $[(TMTMP)Fe(IV)=O]^{+\cdot}$ suggest that the unpaired electron occupies an a_{1u} orbital. The solution magnetic susceptibility measurement by the NMR Evans' method for $[(TMTMP)Fe(IV)=O]^{+\cdot}$ yielded a value of $\mu_{eff} = 3.8 \pm 0.2\ \mu_B$ at –80°C which is consistent with an $S = {}^3/_2$ system [39].

The so-called "push" effect in the hydrolysis of the dioxygen molecule by iron-porphyrin complexes (electron donation from the ligand *trans* to O_2) has been investigated by time-resolved low-temperature UV-VIS and NMR spectroscopy [40]. The reaction of *m*-chloroperbenzoic acid with hydroxo-Fe(III)(2,6-dimethylphenylporphyrin) in the presence of 1-Me-5-Cl-imidazole, 1-phenyl-imidazole or 1-methylimidazole was found to yield a six-coordinated ferric low-spin complex which was found to accelerate dioxygen cleavage when compared to the reaction of the porphyrin with the peracid in the absence of imidazole.

The reaction of $[Fe(TPP)(OMe)_2]^-$ with *tert*- or n-butylhydroperoxide in dmso has been studied by ESR, optical and NMR spectroscopies [41]. Under aerobic conditions, ESR and NMR spectroscopic measurements indicate that the diamagnetic species $[Fe(TPP)(OMe)_2]^{2-}$ is produced; this is believed to be in the low-spin (S = 0) ferrous state. Low-temperature ESR and optical spectral measurements indicate the presence of the intermediate [Fe(TPP)(OMe)(OOBu)], in which the deprotonated peroxide anion binds at the axial position.

The water soluble iron(III) (*meso*-tetrakis(pentafluorophenyl-β-tetrasulfonatoporphyrin) catalyses the selective oxidation by magnesium monoperoxyphthalate (MMP) of H_2O_2 of 1,2-dimethoxyarenes bearing electron withdrawing substituents to muconic dimethyl esters. This novel reaction provides a one step access to muconic dimethylesters bearing various functions in β-positions [42]. A possible mechanism (Scheme 2) would involve (*i*) the formation of a radical cation of dimethoxyarene and a Fe(IV)=O species with a possible Fe(V)=O intermediate, (*ii*) addition of H_2O at the cationic site and Fe(IV)=O at the radical site of dimethoxyarene$^{+\cdot}$ leading to the formation of a Fe(III)-cyclohexadieneolate, (*iii*) oxidation of the Fe(III)-cyclohexadieneolate by MMP, and (*iv*) cleavage of the C-C bond of the Fe(III)-cyclohexadieneolate.

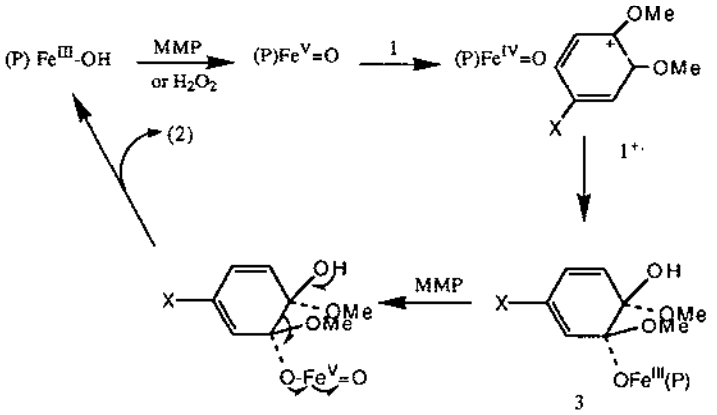

Scheme 2. *A possible mechanism for selective oxidation of 1,2-dimethoxyarenes by iron-porphyrin complexes. Adapted from* [42].

Assignments of ν(HO-Fe-OH) have been made for both the high and low spin bis-hydroxoiron(III) complexes containing TMpyP (tetrakis-5,10,15,20-(2-N-methylpyridyl)-porphinato) at pH 12. Above pH 11 the Fe(III) complex mimics the hemes of alkaline metmyoglobin and methemoglobin in that both the high and low spin complexes are present in thermal equilibrium at room temperature [43].

The iron(III) derivatives of tetrasodium *meso*-tetrakis(*p*-sulfonatophenyl)porphyrin and of $TMpyPH_2$ have been found to be potent catalysts for the chemiluminescent oxidation of luminol or isoluminol [44]. The luminescence produced at pH 7.5 in the presence of isoluminol, H_2O_2 and the water-soluble ferric porphyrin complexes was found to be in the same order of magnitude as that produced by horseradish peroxidase under the same conditions.

The oxygen atom of $[Fe(OEP)]_2O$ may be protonated with $HClO_4$, thus forming the first example of a bridged diiron(III) complex with an unsupported hydroxide bridge $\{[Fe(OEP)]_2(OH)\}^+$ (**38**). The crystal structure of the complex reveals that the two porphyrin rings are almost eclipsed. The complex exhibits a strongly blue-shifted Soret band (λ_{max} = 361.7 nm in CH_2Cl_2) [45].

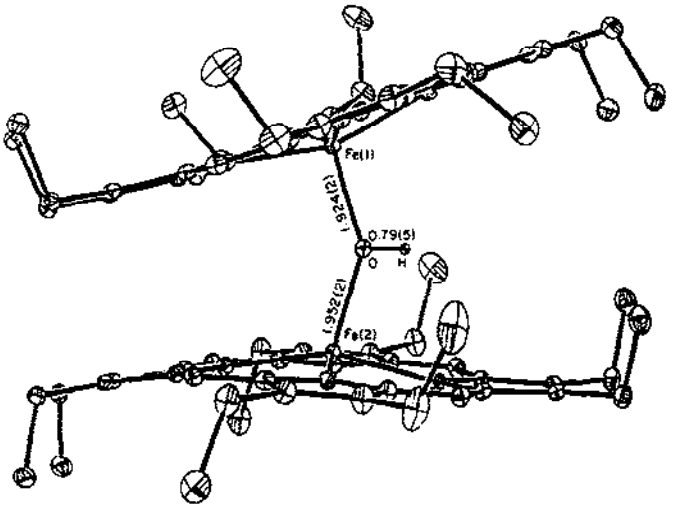

Crystal structure of **38**.

3.5.2.3 Strapped porphyrin complexes

Sterically distorted Fe-CN bonds created by "strapped" iron(II) porphyrins exhibit a large upfield shift in the cyanide ^{15}N NMR spectroscopic signal, making steric effects an important consideration in interpreting the ^{15}N NMR spectra of cyanomet haemoproteins [46]. The changes in the ^{15}N NMR isotropic shift of cyano-haemo complexes arise from interactions between the Fe(III) and $C^{15}N^-$ taking place through bonds and space. The bending of one cyano ligand caused by the shortening of the strap reduces μ, an energy gap. A decrease in μ causes decrease in the magnetic anistropy, which results in an upfield shift for both cyano nitrogens bound to the iron. The $(C^{15}N)_2Fe$ strap porphyrin where the strap is a four carbon chain shows peaks 503 and 386 ppm, an upfield shift of 239 and 357 ppm with respect to the corresponding non-strapped porphyrin.

The influence of the steric bulk of the imidazole ligand of strapped porphyrin hemoglobin-like (a variation of $TPivPPH_2$) complexes has been probed by FTIR and ^{17}O NMR spectroscopies. When imidazole is substituted by the sterically more bulky 1,2-dimethylimidazole, the ^{17}O-resonances of the bound dioxygen molecule are shifted by 30-40 ppm, consistent with a longer

Fe-O bond, whereas the N-H stretch of the "picket" amides does not indicate hydrogen bonding between this moiety and O_2 [47].

Synthesis and X-ray structure of a doubly strapped porphyrin are reported. A simple diamido-alkyl chain (-O(O)C-$(CH_2)_{10}$-CO-) straps one face of the macrocycle while a diamido pyrene unit containing a planar pyrene protects the other face. This pyrene unit is 4.93 Å from the centre of the nitrogen mean plane of the porphyrin. Preliminary binding studies suggest the diamido-pyrene strap reduces the affinity for CO relative to that of O_2 [48].

A ferric complex of a C_2-chiral 1,4-xylylene-strapped porphyrin (**39**) has been utilized for the asymmetric oxidation of aryl sulfides. The FeCl-complex of the ligand was used to oxidize several thioethers, using iodozobenzene as the oxidant. It was found that the enantioselectivity was promoted by the presence of imidazole. Reported enantiomeric excesses vary from 18-71 % [49].

Asymmetric epoxidation of aromatic olefins has been achieved using a BINAP-functionalized ferric porphyrin (**40**) as a catalyst. A tetraether macrocycle was synthesized by linking two binaphthol molecules *via* two 2,4-methylenebenzoethyl ester moieties which in turn are linked to two o-aminophenyl substituents of the porphyrin ring to yield a molecule with D_2 symmetry. The enantiomeric excesses reported vary from 21-63 % [50].

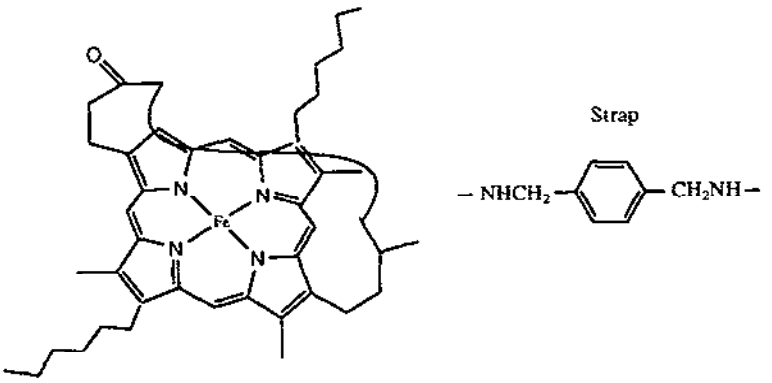

(**39**)

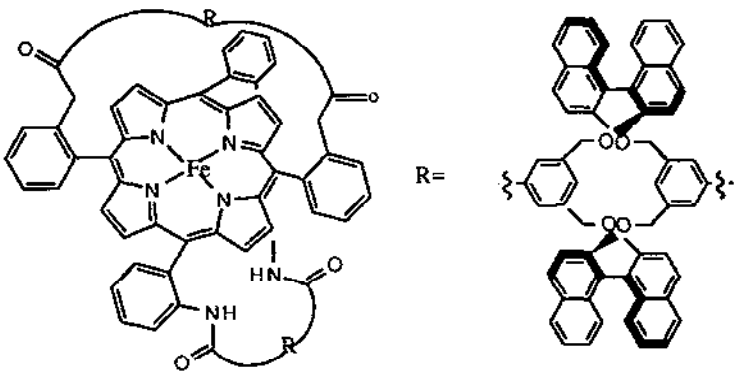

(**40**)

On reaction with *O*-donors or O_2, the doubly bridged iron porphyrinates with thiolate ligands undergo O-insertion at a nonactivated C-H bond of the covalently bound substrate. The mechanism of O-insertion with O_2 most likely involves homolytic cleavage of the O-O bond followed by O insertion *via* radical recombination [51]. The reaction of the Fe(III) porphyrin (**41**) with PhIO, $C_6F_5(IO)$, t-BuOOH, or 3-$CCl_3C_6H_5CO_3H$ produced a significant bathochromic shift of the Soret band from 412 to 418. The mass spectra of the products clearly domonstrated mono-O-insertion at the alkane bridge spanning the porphyrin face opposite to the thiolate ligand.

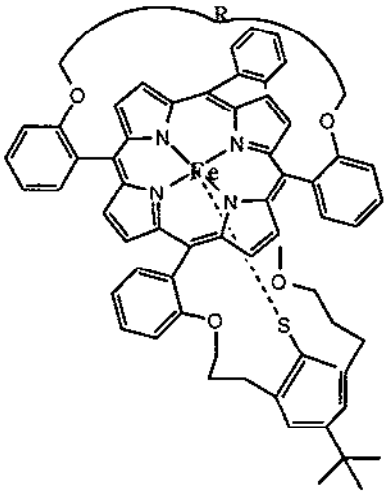

R=C_{11}

(41)

3.5.2.4 Other porphyrin complexes

Mössbauer spectroscop icmeasurements on [Fe(OEP·)]Cl show a large quadropole splitting in the zero-field spectrum, indicative of an admixed intermediate-spin state, rather than the previously assumed high-spin state. Fitting of mixed-spin models to Mössbauer and magnetic susceptibility data indicate a 16-30% admixture of an S = $^5/_2$ state in the S = $^3/_2$ ground state [52].

Crystallographic and NMR spectroscopis results are reported for [Fe(**42**)Cl] where (**42**)H_2 = 2,7-dioxo-3,3',8,8',12,13,17,18-octaethylporphyrin). The ferric complex serves as a model for heme d_1, the unusual dioxoisobacteriochlorin (iBC = isobacteriochlorin) prosthetic group of bacterial dissimilatory nitrite reductases. The coordination and displacement of the iron atom in [Fe(**42**)Cl] are similar to those found in pentacoordinate, high-spin iron(III) porphyrins, as is the domed conformation of its macrocycle. The keto groups appear to be in conjugation with the iBC π system and thereby minimize the distinctive characteristics of the iBC which are normally harder to reduce and easier to oxidize than porphyrins. Crystallographic results for the free base (**42**)H_2, although at poorer precision than for [Fe(**42**)Cl], indicate that the NH protons are localized on adjacent pyrrole rings, and that the macrocycle is not inherently ruffled to any significant extent [53].

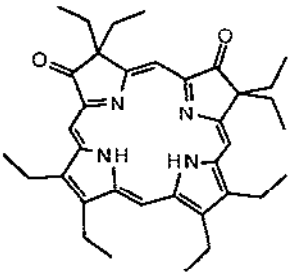

(42)

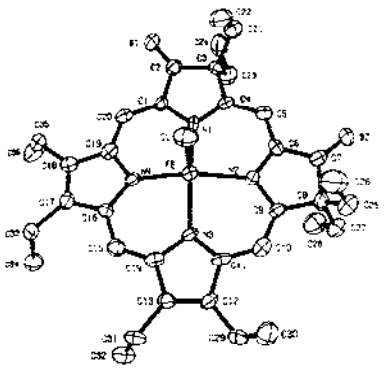

Crystal structure of Fe(42)Cl.

The bis(1-methylimidazole)iron(II) complexes of porphyrins substituted with trifluoromethyl groups exhibit the splittings of Q-bands in the electronic spectra [54]. The splittings may arise from asymmetric electronic effects of the highly electron withdrawing CF_3 group on the porphyrin periphery. The MCD spectra in the Soret region changes in shape with the number of trifluoromethyl groups on the porphyrin.

A series of phenylene-bridged bis-porphyrin adducts containing one, two, or three C_6H_4 bridges (**43**) have been synthesized. The rigid phenyl units allow for edge to edge separations of 5.8 to 14.1 Å. Mixed metal complexes, with Zn in one porphyrin macrocycle and Fe(III)(bis-imidazole) in the other macrocycle, have been prepared for studies of photochemical electron transfer. When photoexcited, an electron is transferred from Zn to Fe(III). The rate of this process drops only slowly with distance; it is proportional to $\exp(-\beta r)$, with $\beta = 0.4$ Å^{-1}. The dependence can be predicted by a theory which assumes that the drop does not reflect increased distance, but rather reflects the break in conjugation which occurs at each Ph juncture due to the biphenyl twist angle of approximately 50° [55].

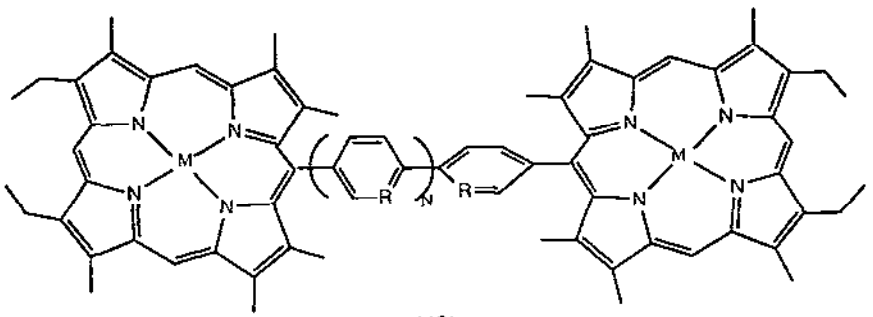

(43)

The kinetics of photolysis and recombination of geminate pairs have been studied for a number of Fe(II)hemes (protoheme, protoheme dimethyl ester, protoheme methyl ester and protoheme stearyl ester) as well as a number of ligands. The relaxations are on the ps scale; the

kinetics show clear first-order processes. Geminate return of carbon monoxide to 1-methylimidazole-protoheme in glycerol is considerably slower (3×10^9 s^{-1}) [56].

Picosecond photolysis has been used to probe the ligand dissociation from protoheme dimethyl ester $(CNR)_2$ (R = Me, ^{t}Bu) complexes. It is found that loss of one isocyanide produces an electronically excited five-coordinated species which rapidly (< 40 ps) decays to a ground-state five-coordinated heme. In contrast to similar imidazole-heme species, the return to heme$(CNR)_2$ species is a relatively slow concentration-dependent process. With larger isocyanides, such as 5α-cholestan-3α-isocyanide and the 3β isomer, the excited states return to the 6-coordinated state with only a few percent of ground-state 5-coordinated heme formation. This behaviour is attributed to a faster decay of the excited state resulting from an interaction of the heme with the cholestane backbone. It is concluded that excited-state 5-coordinated hemes do not add ligands [57].

The effect of pressure on the reaction of chelated protoheme with carbon monoxide in mineral oil/toluene solutions was investigated to determine whether the appropriate combination of solvent viscosity and hydrostatic pressure can induce a change in the rate determining step of a bimolecular reaction. Increasing hydrostatic pressure from 1 to 3000 atm in toluene solutions of chelated protoheme-carbon monoxide resulted in an increase in the bimolucular rate of CO geminate recombination after photolysis of the complex. When the same series of kinetic measurements were made in the more viscous solvent mineral oil, the bimolucular combination rate increased with pressure up to about 1000 atm and decreased over the range of 2000-3000 atm. These results indicate a change of the rate limiting step from bond formation to diffusion as the pressure is increased and they suggest that the CO binding mechanism differs significantly from those of all other simples ligands. Carbon monoxide reacts with 5-coordinated heme compounds with activation control at low viscosity. Other ligands such as isocyanides and imidazoles react with diffusion controlled rates [57a].

Hydroxylation of norbornane and tetra-exo-deuterionorbornane using iron(III) tetrakis(2,6-dichlorophenyl)octabromoporphyrin afforded good yields of products which consisted of 86:13:<1 and 84:16:<1 ratios of exo-norborman-2-ol, endo-norborman-2-ol, and 2-norbornanone, respectively. In the latter case, both D3 and D4 *exo* and *endo* alcohols but only D3 ketone were obtained. The primary isotope effect is 5. These results show that the reaction involves loss of stereochemistry and agree with those from a previous study using cytochrome P 450. As in that case, this hydroxylation proceeds through a free-radical cage process. An intermediary carbocation is not involved in the mechanism. The hemin catalysis leads to a loss of stereospecificity similar to that in the enzyme-catalysed reaction [58].

3.5.3 Complexes with chlorins

Chemical oxidation of iron(II) nitrosyl complexes of octaethylchlorin ($OECH_2$) and octaethylisobacteriochlorin ($OEiBCH_2$) yielded iron(II) nitrosyl π-cation radicals as evidenced by the ^{1}H and ^{2}H NMR spectra of selectively deuterated [(OEC)Fe(II)NO] complexes. Downfield shifts indicative of a ligand-based radical were observed. Comparison of the relative downfield shifts of the chlorin macrocycles with calculated electron densities suggests an a_2 radical state. The

temperature-dependence of the isotropic ^2H shifts of the two complexes do not follow non-Curie law behaviour and is interpreted in terms of a valence isomerization from the chlorin π-cation radical to the Fe(II)NO^+ chlorin complex due to ligation of $[SbF_6]^-$ to the iron of the π-cation radical as well as a magnetic interaction between the NO and π radical spins in [(OEiBC)Fe(II)NO] π-cation radical. This valence isomerization was confirmed by variable-temperature electronic absorption spectral measurements. Ligation of imidazole to the π-cation radicals caused valence isomerization to yield [(OEC)Fe(II)(NO^+)(Im)] and [(OEiBC)Fe(II)(NO^+)(Im)] complexes [59].

An oxoiron(IV) chlorin π-cation has been synthesized from the oxidation of [(TMC)Fe(III)(*m*-chlorobenzoate)] ($TMCH_2$ = 7,8-dihydro-5,10,15,20-tetrakis(mesityl)porphin, **(44)** by *m*-chloroperoxybenzoic acid. Deuterium NMR spectroscopic measurements on the deuterated [(*m*CB)OFe(IV)(TMC^+)· show three pyrrole D resonances with large upfield shifts and the *meta* D resonance exhibits a small downfield shift which implies small spin densities at the meso carbons of the chlorin ring. The oxoiron(IV) π-cation species is unstable on the NMR spectroscopic time scale even at –80°C and is EPR silent at 77 K. Upon addition of norbornene to the π-radical solution, the UV-VIS spectrum showed no changes within 3 hours while the corresponding porphyrin π-cation radical reacted to give norbornene oxide in 3 hours. It appears that chlorin π-cation radicals of the a_2 (a_1u) type exhibit lower reactivity towards alkenes than the corresponding a_{2u} type porphyrin π-cation radicals [60].

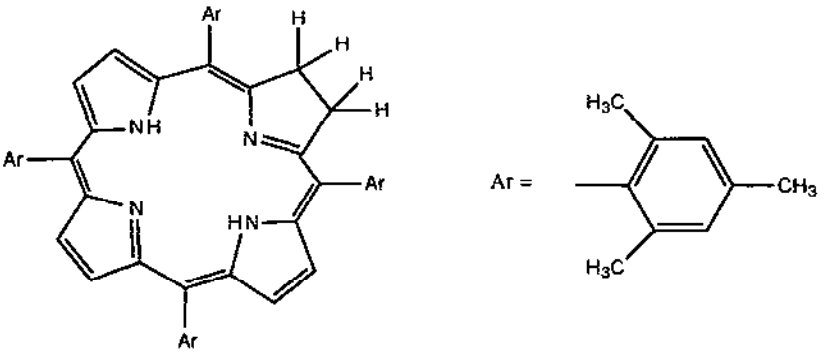

(44)

The voltammetry and spectroelectrochemistry of [Fe(TPC)]Cl and [Fe(TPiBC)]Cl, where $TPCH_2$ = tetraphenylchlorin and $TPiBCH_2$ = tetraphenylisobacteriochlorin, were studied in ethylene chloride and tetrahydrofuran. The reduction of both complexes yielded iron(II) and iron(I) complexes. The oxidation of [Fe(TPC)]Cl and [Fe(TPiBC)]Cl led to the formation of Fe(TPP)Cl. The most probable mechanism is the dehydrogenation of the π cation radical formed by the oxidation of the hydroporphyrin rings. The first reduction for both complexes was found to be reversible in cyclic voltammetry while the second was reversible only for Fe(TPC)Cl. The $E_{1/2}$ values for the first and second reductions were independent of the identity of the macrocycle. The first reduction occurred at the same potential as Fe(TPP)(NO) and Fe(TPC)(NO) [61].

3.5.4 Miscellaneous tetrapyrrole complexes

In order to find diagnostic signatures for biological hydroporphyrins, the resonance Raman spectra of model chlorins (dihydroporphyrins), porphyrindiones (dioxoporphyrins), and isobacteriochlorins ($iBCH_2$; tetrahydroporphyrins) have been investigated. Several octaethylisobacteriochlorin ($OEiBCH_2$) complexes have been studied, including solid-state, S = 1, tetracoordinate Fe(II)octaethylisobacteriochlorin [Fe(OEiBC)], [(NCS)Fe(III)(OEiBC)], $[(Me_2SO)_2Fe(II)(OEiBC)]$, $[(Im)_2Fe(III)(OEiBC)]$, $[(2\text{-Me-Im})_2Fe(II)(OEiBC)]$ and $[(py)_2Fe(II)(OEiBC)]$. High-frequency ($\geq$ 900 cm^{-1}) RR spectra of FeOEiBC are clearly distinct from those of high-spin pentacoordinate or low-spin hexacoordinate ferrous porphyrin, chlorin, or iBC complexes. Rather, the spectral features of Fe(OEiBC) are at frequencies typical of low-spin, hexacoordinate ferric porphyrin, chlorin, and iBC model complexes. There are spectral features that distinguish each type of macrocycle. For porphyrins, these are: a single polarized band in the oxidation-state region (≈1340-1400 cm^{-1}) and a depolarized ν_{10}>1600 cm^{-1}, well known to be sensitive to spin-, coordination-, and oxidation state. For chlorins, this includes a strong polarized ν_{10}-equivalent >1600 cm^{-1}, which is also the IR-active "chlorin band". For iBCs, this includes a strong, polarized ν_{29}-equivalent at ≈1400 cm^{-1}, not responsive to ^{15}N 4-substitution. The iBC "marker band" increases in relative intensity on going towards visible excitation [62].

3.6 COMPLEXES WITH OXYGEN DONOR LIGANDS

3.6.1 Complexes with carboxylic acids and derivatives

The oxidation of $[Fe_2(ttha)(H_2O)_2]^{2-}$ (H_6ttha = triethylenetetraminehexaacetic acid) by H_2O_2, yields $[Fe_2O(ttha)]^{2-}$, the tetranuclear complex $[Fe_4(O)_2(ttha)_2]^{4-}$, and traces of $[FeCl_4]^-$ and $[Fe(tthaH)]^{2-}$ [63]. The oxidation reaction is only slightly inhibited by tert-BuOH; this indicates that OH radical production is not a major pathway in the reaction. The oxidation is proposed to occur via formation of ferryl species which react with a second Fe(II) either via an inner-sphere mechanism to form $[Fe_2O(ttha)]^{2-}$ or an outer-sphere mechanism to form the linear chain complex $[Fe_2(ttha)(OH_2)_2]$.

The reaction of $[Fe(H)(\eta^1\text{-}N_2)(P(CH_2CH_2PPh_2)_3)](BPh_4)$ with pentynoic acid affords the carboxylate complex $[Fe(O_2CCH_2CH_2CCH)(P(CH_2CH_2PPh_2)_3)](BPh_4)$, (**45**)$(BPh_4)$, the crystal structure of which has been determined. The carboxylic oxygen atoms have a weaker *trans* effect than the phosphine ligand(s). Thus, both Fe-P bonds *trans* to the oxygen atoms are slightly shorter than the other two [64].

The structure of bis(dipicolinato)ferrate(III) dihydrate (**46**) has been determined. The Fe-N and Fe-O bond distances of the two orthogonal picolinate ligands are slightly different [65].

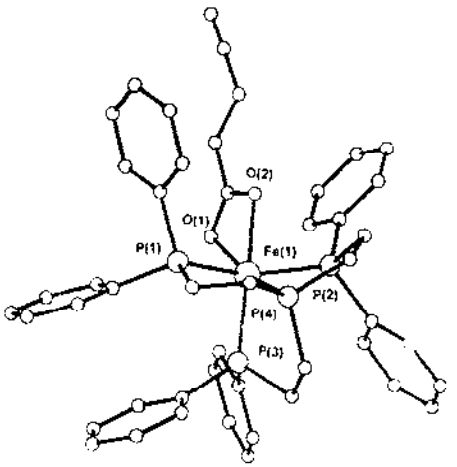

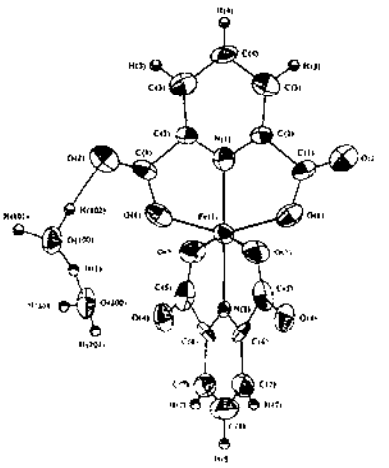

(45) (46)

Crystal structures of (45) and (46).
Reprinted with permission from [64] and [65]. Copyright International Union of Crystallography.

3.6.2 Complexes with other O-donor ligands

Enterobactin analogs, based on 1,3,5-tris(aminomethyl)benzene (tram) (47) and on tris(2-aminoethyl)amine (tren) (48) as anchors and an amino acid linking the anchor to the catechol residues, have been prepared. The ligands form 1:1 complexes with iron(III). Their configurations were examined by CD spectroscopy and were found to be Δ-*cis* (similar to enterobactin) for all L-amino acid-based ligands with the exception of the N-methylated L-leu derivative of tram. D-amino

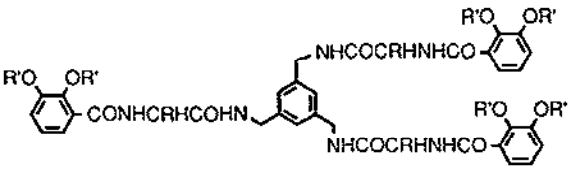

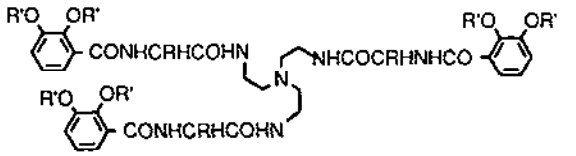

(47), top and (48), bottom.

acid based ligands adopted the Λ-*cis* configuration. The tram catechoylamides 1,3,5-[2,3-$(HO)_2C_6H_3CO$-X-$NHCH_2]C_6H_3$ (X = L-Leu (**49**), L-Ala, D-Ala) adopt random conformations in protic solvents, while the corresponding tren catechoylamides [2,3-$(HO)_2C_6H_3CO$-X-$NHCH_2CH_2]_3N$ (l; X = L-Leu, L-Ala) form H-bonded structures under analogous conditions. The L-Leu derivative of tren was the most efficient Fe^{3+} ion binder so far prepared, approaching enterobactin's binding constant. This may be due to the relatively small entropy change for the ligand upon coordination to the metal [66].

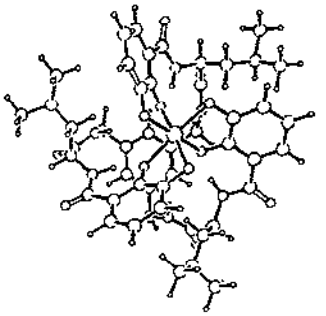

Calculated structure of **49**.

The crystal structure of Fe(1-ethyl-3-hydroxy-2-methylpyridin-4-one)$_3 \cdot 3\ H_2O$ has been determined and compared to the analogous 1-butyl-3-hydroxy-2-methylpyridin-4-one complex. It is found that the carbonyl bond of the ligand (**50**) lengthens while the hydroxyl bond shortens when changing from the ethyl-substituted to the butyl-substituted ligand. This is interpreted as an indication of greater stability of the ethyl-substituted complex [67].

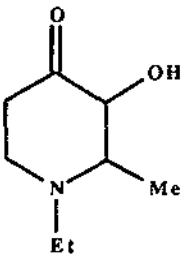

(50)

Reaction of $Fe(N(SiMe_3)_2)_2$ with 3,5-di-^{t}butylcatechol ($DBCatH_2$) in pyridine yields $[Fe_2(DBcat)_2(py)_n]$ (n = 4 (**51**), 6). If the reaction is carried out in toluene or hexane, addition of pyridine results in the formation of the complex $[Fe_4(DBCat)_4(py)_6]$ (**52**). All three compounds have been characterized by X-ray crystallography [68].

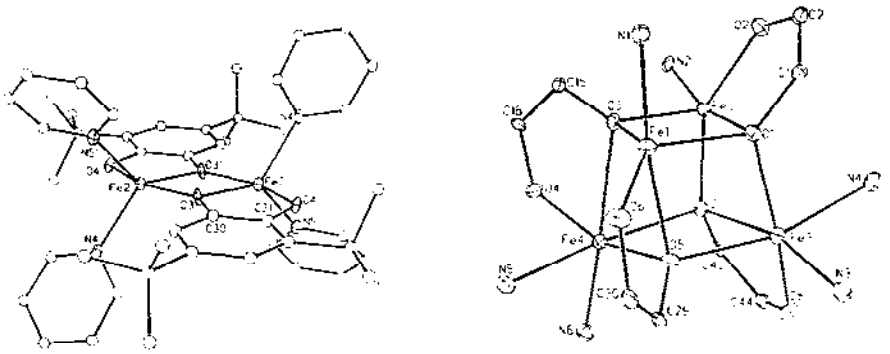

Crystal structure of **(51)** (left) and **(52)** (right).

The crystal structure of $[Fe(acac)_2(OCH_2CF_3)]_2$ has been determined and its magnetic susceptibility measured in the temperature range 4.2-292 K using the Faraday method [69]. The magnetic data were fitted to yield an antiferromagnetic coupling constant ($J = -6.5$ cm^{-1}). This is significantly lower than that of the corresponding ethoxo-compound ($J = -11$ cm^{-1}); it is attributed to the electron-withdrawing effect of the trifluoromethyl group of the alkoxo bridges.

Reaction of an acetonitrile mixture of hexafluoroacetylacetone (hfacH) and the corresponding tetraol 1,1,1,5,5,5-hexafluoro-2,2,4,4-tetraol ($hptH_4$) with $[Fe_3O(OAc)_6(py)_3](ClO_4)$ results in formation of the mononuclear $[Fe(hfac)_2(hfptH_2)](pyH)$ **(53)** whose crystal structure is shown [70].

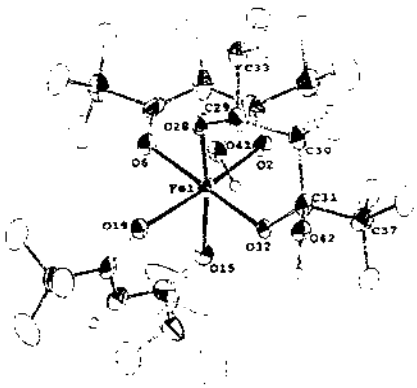

Crystal structure of **(53)**.

Tris(4-diphenylphosphinoyl-3-methyl-1-phenylpyrazol-5-onato-*O*,*O*')iron(III) **(54)** has been synthesized by the reaction of $Fe(NO_3)_3$ with the conjugate acid of the ligand in water. The crystal structure of **(54)** has been determined, and both the Δ and the Λ configurations are found in the unit cell [71].

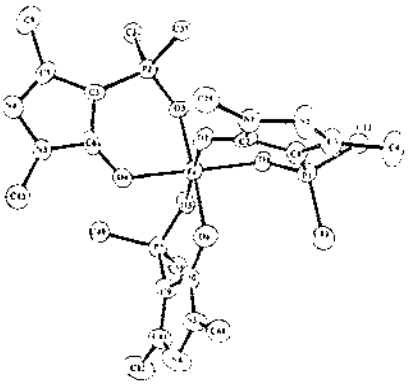

Crystal structure of (54).

3.7 COMPLEXES WITH SULFUR DONOR LIGANDS

The reaction of ferrous halides with the macrocyclic thioethers (14)aneS$_4$ and (16)aneS$_4$ ((14)aneS$_4$ = 1,4,8,11-tetrathiocyclotetradecane, (16)aneS$_4$ = 1,5,9,13-tetrathiocyclohexadecane) in MeCN results in the formation of [Fe(MeCN)$_2${(14)aneS$_4$}][FeI$_4$] and [Fe{(16)aneS$_4$}]X$_2$ (X = Br, I) (55) [72]. Whereas the Mössbauer spectrum at 77 K of the former compound is consistent with a low spin octahedral iron(II), those of the (16)aneS$_4$ adducts exhibit large quadropole splittings (X = Br, Q = 3.60 mm s^{-1}; X = I, Q = 4.10 mm s^{-1}). The magnitude of these splittings, in combination with the isotope shifts and the measured magnetic moments (μ_{eff} = 5.8 for X = Br and 5.1 for X = I) are consistent with high spin Fe(II). The large Fe-I distances (2.89 Å) in the complex are close to the sums of the ionic radii of high spin Fe(II) and I, and the compound may be viewed as containing a square planar Fe(II) centre. It is proposed that this geometry is caused by ring strain in the macrocycle. Attempts to reduce the ((16)aneS$_4$) iron adducts to Fe(0) resulted in decomposition of the complexes.

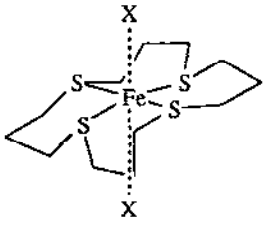

(55)

Complexes containing [Fe(C$_3$S$_5$)$_2$]$^-$ and [Fe(C$_3$Se$_5$)$_2$]$^-$ (H$_2$C$_3$S$_5$ = 4,5-dimercapto-1,3-dithiole-2-thione, H$_2$C$_3$Se$_5$ = 4,5-di(hydroseleno)-1,3-diselenole-2-selone) have been prepared. Single-crystal X-ray analyses of the [NBu$^n_4$]$^+$ and [Fe(Cp)$_2$]$^+$ salts of [Fe(C$_3$Se$_5$)$_2$]$^-$ revealed

dimerized geometries for the anions with square-pyramidal coordination around each Fe(III) through intermolecular Fe-S linkages. Short Fe-Fe distances (3.17Å) for $[NBu^n_4][Fe(C_3S_5)_2]$ result in strong antiferromagnetic interactions between metal centres. Values of binding energies for the oxidized $[Fe(C_3S_5)_2]^{n-}$ are almost the same as those of unoxidized $[Fe(C_3S_5)_2]^-$ species indicating ligand centreed oxidation. The binding energies of the $[Fe(C_3S_5)_2]^{n-}$ complexes are similar to those of the selenium analogues; however, the unoxidized $[Fe(C_3S_5)_2]^-$ species exhibits lower binding energies. The strong Fe-S interactions, as well as the difference in geometry around the Fe(III) ion, may result in lowering of the binding energy [73].

The reaction of (R_4N)[Fe(2,6-dimethylphenolate]$_4$ (R = Et, ^{n}Pr), with excess RSH (R = Me, Et, ^{i}Pr, Ph) in concentrated dmf solutions at 0°C result in the formation of the corresponding ferric tetrathiolate complexes, which are synthetic analogues of oxidized rubredoxin iron centra. The crystal structures of $[Fe(SR)_4]^-$ (R = Me, Et, Ph) have been determined; that of $[Fe(SEt)_4]^-$ (**56**) is shown [74].

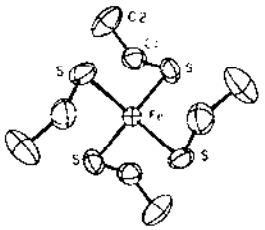

Crystal structure of (**56**).

3.8 COMPLEXES WITH PHOSPHORUS DONOR LIGANDS

Addition of 1,3-bis(dimethylphosphino)propane (dmpp) to a toluene-ethanol-suspension of $FeCl_2$ affords the green *trans*-$[Fe(dmpp)_2Cl_2]$ whose crystal structure has been determined. The ligand is easily displaced by dmpe. Reduction of $[Fe(dmpp)_2Cl_2]$ with $LiAlH_4$ results in the orange-brown $[Fe(dmpp)_2HCl]$ which can be further reduced to the corresponding dark yellow dihydride species [75].

3.9 COMPLEXES WITH MIXED-DONOR LIGANDS

3.9.1 Complexes with mixed N,O-donor sets

Magnetic studies and Mössbauer spectra measured for the members of the $[Fe(bpy)(Cl_4Cat)_2]^n$ series where n = 0 and n = –1 indicate the metal remains as a high spin ferric ion throughout the series and all redox activity occurs at the quinone ligand [76]. Redox activity occurs from the catecholate π-level which is lower in energy than the iron 3d levels to give the mixed-charge ligand complex. Synthesis of $(PPh_4)[Fe(bpy)(Cl_4Cat)_2]$, (PPh_4)(**57**), is dependent

on the sequence of reagent addition. When Fe^{3+} and PPh_4^+ are reacted in base and then the bpy and Cl_4Cat^{2-} ligands are added, $[Fe(OPPh_3)_3(HCl_4Cat)(Cl_4Cat)]$ (**58**) is formed. Coordination of a protonated catechol is rare.

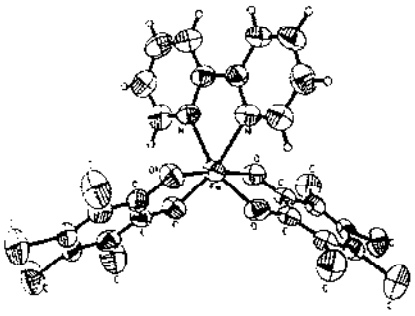

(**57**)

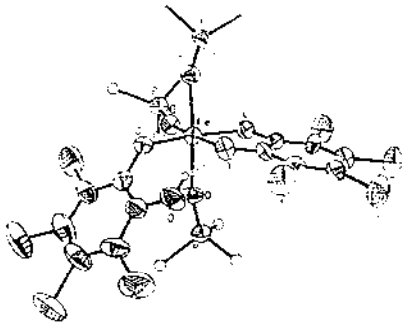

(**58**)

Magnetic hyperfine properties of four spin-coupled (*o*-semiquinonato) iron complexes were compared to the those of the related high spin ferric compound, [Fe(salphen)(catH)] [77]. Analysis of the magnetic susceptibility results showed that the number of unpaired electrons correlates linearly with the hyperfine interaction found at the ^{57}Fe nucleus in the Mössbauer spectroscopic studies. The linear correlation is indicative of a primarily Fermi contact interaction between the unpaired electrons and the ^{57}Fe nucleus which is expected for a high spin ferric ion.

The complexation towards iron of the tridentate trianionic chelating ligand, *N*-(2-hydroxyphenyl)salicylamide (H_3L^1, (**59**)) and its homologues with a substituent on the 2-hydroxyphenyl moiety (5-CH_3, H_3L^2; 5-Cl, H_3L^3), has been studied [78]. The ligand H_3L^1 was found to form a high-spin iron(III) complex $K_3[Fe(L^1)_2]$ when treated with $FeCl_3$ in an alkaline solution under aerobic conditions. This complex may be oxidized with Ce(IV) to a high-spin iron(IV) complex $(NPr_4)_2[Fe(L^1)_2]$. The ligand H_3L^2 forms a low-spin iron(IV) complex $K_2[Fe(L^2)_2]$ under aerobic conditions whereas the ligand H_3L^3 gives the high-spin iron(III) complex $(PBu_4)_3[Fe(L^3)_2]$. The most donative ligand $([L^2]^{3-})$ formed the low spin (IV) complex while the the least donative $([L^3]^{3-})$ afforded only an iron(III) complex. The parent ligand (**59**) which is moderately donative formed both iron(III) and (IV) complexes. The iron(IV) complexes from ligand $[L^1]^{3-}$ and $[L^2]^{3-}$ are of different spin states.

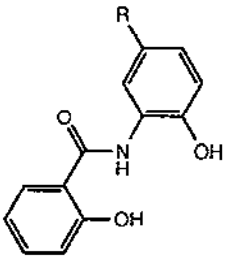

(**59**)

The ligand *N,N',N,N'*-bis[(2-hydroxybenzyl)(2-methylpyridyl)]-2-ol-1,3-propanediamine (H_3BBPPNOL) (**60**) has been used to synthesize a dinuclear μ-alkoxo, μ-carboxylato iron complex [79]. The Mössbauer and UV-VIS spectral properties of the compound are similar to those of the iron-containing purple acid phosphatase enzymes.

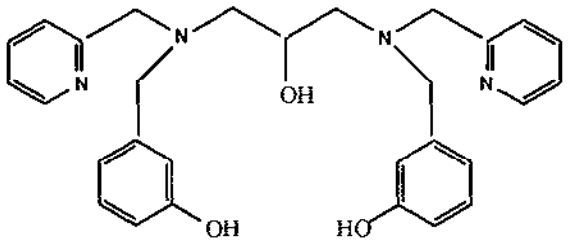

(**60**)

Iron-induced activation of H_2O_2 or ^tBuOOH has been has been used for catalytic monooxygenation, ketonization and dioxygenation [80]. The metal complexes used were $Fe(II)(PA)_2$ (PA = anion of picolinic acid), $Fe(II)(DPA)_2^{2-}$ (DPA = dianion of 2,6-pyridinedecarboxylic acid), $FeCl_3$, $[Fe(II)(OPPh_3)_4](ClO_4)_2$, $[Fe(II)(bpy)_2](ClO_4)_2$ and $[Fe(NCMe)_4]^{2+}$. When the HOOH/ML ratio is at least 10, all of the complexes catalytically ketonize methylenic carbons and dioxygenate aryl olefins. The most effective catalyst systems were found to be $Fe(II)(PA)_2/py_2(HOAc)$ and $[Fe(II)(OPPh_3)_4]^{2+}$/MeCN. The reactive intermediates are proposed to be iron hydroxo/hydroperoxo complexes such as $(PA)_2Fe(IV)(OH)(OOH)$.

The ligand *N,N'*-bis(2-hydroxybenzyl)ethylenediamine-*N,N'*-dipropionic acid (HBEP) (**61**) has been synthesized and reacted with $Fe(NO_3)_3$ to form $[Fe(HBEP)]^-$ [81]. The stability constant of this complex is slightly lower that the corresponding *N,N'*-bis(2-hydroxybenzyl)ethylenediamine-*N,N'*-diacetate (HBED) chelate.

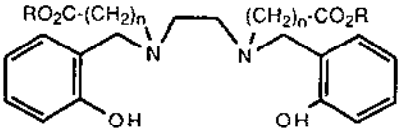

(**61**)

The bridged complex μ-(terephthalato)bis[*N,N'*-ethylenebis(salicylaldiminato)iron(III)] has been crystallized and its structure determined by X-ray crystallography (**62**) [82]. Magnetic studies show no evidence of an antiferromagnetic exchange between the two iron centres, in spite of the fact that such an interaction is found in the analogous [{(Fe(salphen)}$_2$(μ-ter)] complex.

The diarylphosphinic acid 4,4'-(hydroxyphosphinylidene)bis-L-phenylalanine has been used to coordinate FeX_2 through the amino acids. Each diarylphosphinic acid coordinates two metals; metal/phosphinic acid dimers are formed (**63**) [83].

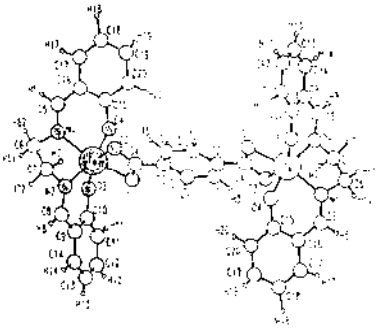

Crystal structure of (62).

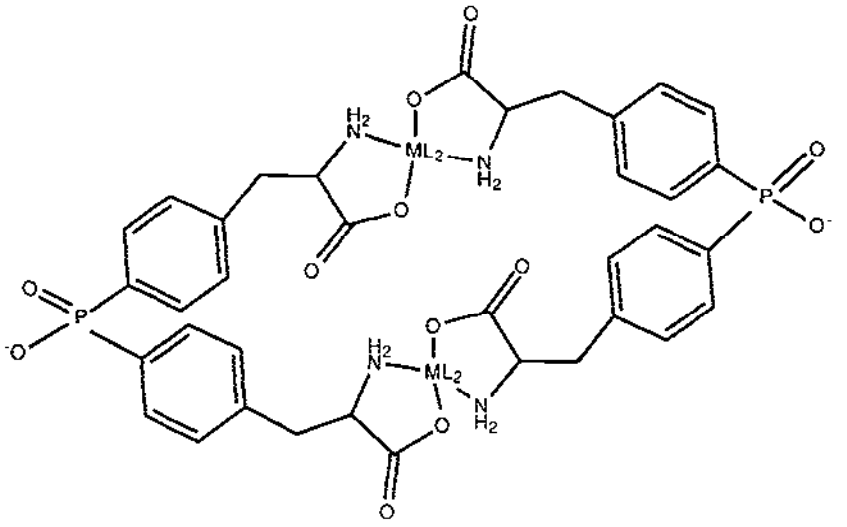

(63)

A nonapeptide with an Ala-(OH)Gly-Ala sequence has been synthesized *via* condensation of appropriately protected tripeptide units [84]. The peptide forms a 1:3 complex of iron(III) with hydroxamate groups at neutral pH when mixed with an aqueous Fe(III) solution. The complex shows an absorption maximun, λ_{max}, at 410 nm at pH 7. Alanine residues influence the hydroxamate groups to produce a chiral complex. The CD spectrum reveals bands at 355 and 435 showing a preference for the Δ configuration around the iron.

A spin crossover complex [Fe(mbpN)(lut)](BPh$_4$) (H_2mbpN = *N*,*N'*-bis((2-hydroxy-5-methylphenyl)phenyl methylene)-4-azaheptane-1,7-diamine (**64**); lut = 3,4-dimethylpyridine), has been reported. The iron ligand bond lengths are close to the average values reported for high spin

complexes. The coordination geometry is similar to that for [Fe(salten)(mpy)](BPh$_4$) which is in almost low spin state except that the ligand configuration is different (**65**). Magnetic susceptibility measurements report a magnetic moment value which is larger than what is characteristic for a low spin Fe(III) but slightly lower than a high spin Fe(III) value. The complex undergoes a faster spin-state interconversion than the lifetime of the ^{57}Fe excited state ($1x10^{-7}$ s). It has been found that the quadrupole splittings of the complex show the lowest value at intermediate spin state transformations [85].

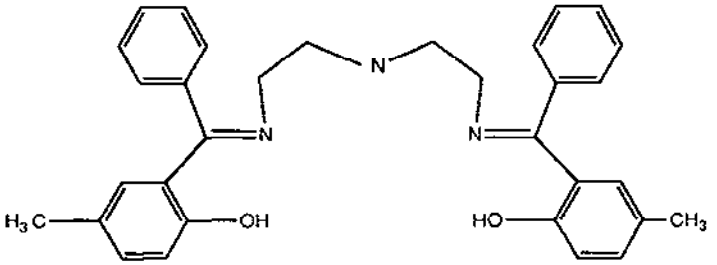

(**64**)

mbpN salten

(**65**)

The stability constants of the ligands 1-oxa-4,7,10-triaza cyclododecane-4,10-diacetic acid (L1) (**66**), 1,7-dioxa-4,10-diaza cyclododecane-4,10-diacetic acid (L2) (**67**), 1,4-dioxa-7,10-diaza cyclododecane-4,10-diacetic acid (L3) (**68**) have been determined by potentiometric titration. Stoichiometric metal-ligand complexes were formed in all cases; in the case of L1, the monoprotonated (N2-H) ligand-metal complex was also identified [86].

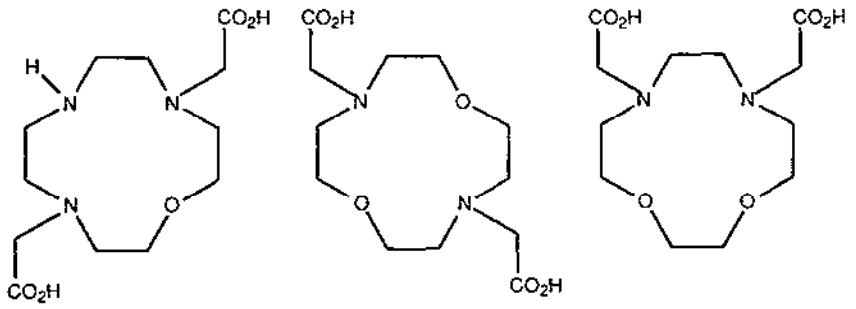

(**66**) (**67**) (**68**)

Iron(III)-phenolate complexes have been studied over the past years due to evidence that Fe(III) ions are bound to a histidine and a phenolate oxygen-atom in the iron transport proteins, transferrin and lactoferrin. Starting from a given macrocyclic ligand (tacn or 1-oxa-4,7-diazacyclononane) as the backbone, six new five- and four- coordinated *N*-phenolate-functionalized ligands (**69**)-(**75**) have been synthesized and reacted with iron(III). The resulting octahedral d^5 high-spin Fe(III) complexes have been studied [87]. It appears that the phenolate to iron(III) charge transfer bands for these complexes are a function of the number of coordinated phenolate ligands. A blue shift of roughly 2000 cm^{-1} is seen. Electron donating substituents in the *ortho-* or *para-*position of the phenolate atom give a bathochromic shift, while electron-withdrawing substituents give a hypsochromic shift. A new dinuclear complex $[L^7{}_2Fe_2(O_2CPh)](ClO_4)_3$ (**76**) (L^7 = *N*-(2-hydroxybenzyl)-1,4,7-triazacyclononane) has been synthesized where the two Fe(III) centres are connected *via* a symmetric benzoate bridge and two phenolate oxygen atoms.

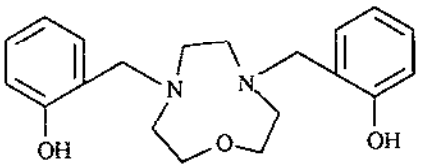

(**69**)

	R^1	R^2	R^3	R^5	R^6
L^2 (**70**)	CH_3	CH_3	R^4	H	H
L^3 (**71**)	CH_3	CH_3	R_4	NO_2	H
L^4 (**72**)	CH_3	CH_3	R^4	H	$C(CH_3)_3$
L^6 (**74**)	R^4	R^4	CH_3	H	H
L^7 (**75**)	H	H	R^4	H	H

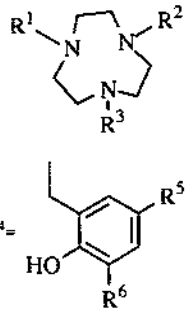

R^4=

L^5 =

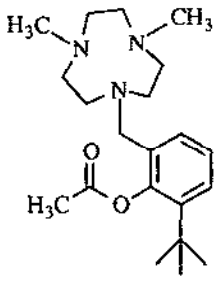

(**73**)

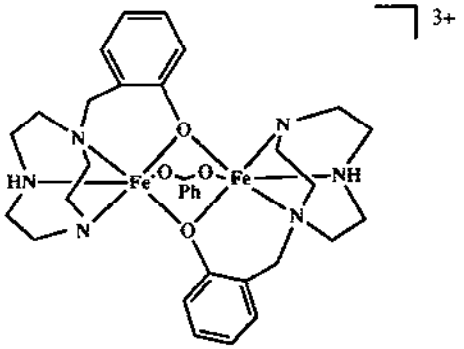

(**76**)

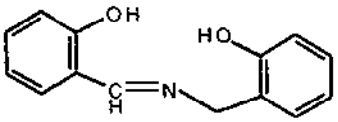

(77)

Reaction of the $FeCl_3$ with H_2salamp (77) and NBu^n_4OH in ethanol affords $NBu_4[Fe(salamp)_2]$ [88]. A series of high-spin octahedral Fe(III) complexes of Schiff bases derived from salicylaldehyde aromatic amines was synthesized. The ligands were selected to encompass various coordination spheres FeN_2O_4, $FeN_2O_2O'_2$, FeN_3O_3 and FeN_4O_2 (O = phenolic oxygen, N = aliphatic or aromatic nitrogen, O' = carboxylate oxygen) to provide generalizations regarding the overall coordination environment of the Fe centre in a closely related group of complexes. They reveal the effect of stereochemistry and/or donor atom variations on the UV-VIS and EPR spectra and Fe(III/II) redox potentials. Information on the Fe(III) site symmetry was obtained by EPR spectroscopic measurements. The optical spectra are largely determined by transitions originating in the Fe-salicylaldiminate chromophore. The ligand-to-metal charge-transfer bands systematically shift to higher energy as the number of phenolate-containing donor sites increases. This blue shift is reflected in more negative Fe(III/II) redox potentials. The order of increasing cathodic potential shift with respect to the coordination sphere is $N_2O_4 > N_2O_2O_2' > N_3O_3 > N_4O_2$. This is a reflection of the decreased Lewis acidity of the Fe(III) centre due to the increase in basicity of the donor atom. A linear spectroelectrochemical correlation was obtained between the phenolate-to-Fe(III) charge-transfer band energy and the Fe(III/II) redox potential. Based on this correlation, trends in the redox potentials of Fe tyrosinate proteins are discussed.

The crystal structures of the iron(III) Schiffs base complexes Fe(acacen)Cl (acacen = *N,N'*-ethylenedbis(acetylacetylideneimine), Fe(acacen)Cl, $K[Fe(acacen)(CN)_2] \cdot 2H_2O$ and $[\{Fe(acacen)\}_2O] \cdot CH_2Cl_2$ have been determined and have been compared to those of the closely related $[Fe(salen)]^+$ complexes [89]. It was found that the acacen complexes exhibit shorter Fe-O bonds and longer Fe-N bonds than the corresponding salen complexes. Furthermore, the acacen complexes exhibit larger variance in the Fe-O, N bond lengths than the salen complexes do: this is presumed to be due to greater steric reqirements of the larger salen ligand.

Schaefer *et al.* report the detection by electrospray-ionization mass spectroscopy of a radical cation present in solution of a tetrahydropteridinone-iron complex [90]. EPR spectroscopic measurements provide evidence that the radical cation existed in solution and was not generated by the electrospray ionization technique. They suggest that this complex might be an Fe(II) radical cation which might be a suitable model complex for the active centre of phenylalanine hydroxylase.

3.9.2 Complexes with mixed N,S-donor sets

Various ferrous complexes of the ligand 2-mercapto-3-pyridinol (PSHOH) have been synthesized by electrochemical means. Reduction of $[Fe(dmu)_6](ClO_4)_2$ (dmu = dimethylurea)

using tetraethylammonium perchlorate as an electrolyte, results in the formation of a dark green species formulated as [{Fe(SHO)$_2${O]. Similarly, reduction of a 1:3 metal/ligand mixtue in the presence of approximately 1.3 equivalents of base (tetramethylammonium hydroxide) per ligand, affords dark blue ([Fe(PSO)(PSHO)$_2$]$^{2-}$; further addition of base (2 moles/ligand) results in the formation of brick red (Fe(PSO)$_3$)$_4$ [91].

The crystal structure of Fe(btz)$_2$(NCS)$_2$ (**78**) (btz = 2,2'-bi-4,5-dihydrothiazine) has been determined by X-ray diffraction at 293 and 130 K in order to detect the structural changes associated with the spin transition that takes place in the complex [92]. The results compare with those reported for Fe(phen)$_2$(NCS)$_2$ although the temperature dependence of the molar magnetic susceptibility is different for the two compounds. The phen compound displays an abrupt singlet-quintet conversion while the btz compound undergoes a more gradual change. When the temperature is decreased from 293 to 130 K, the Fe-N(L) (L = btz, phen) and Fe-N(CS) distances decrease by 0.20 (mean value) and 0.10–0.11) Å, respectively, and a noticeable change of the N-Fe-N angles, leading to a more regular shape of the [Fe-N$_6$] octahedron, is observed. Furthermore, intramolecular interactions due to molecular packing differ between the two compounds. This difference in structural anisotropy might be the origin of the difference in spin transitions and is reflected in the temperature dependence of the lattice parameters. In the btz complex, all parameters change continuously; in the phen complex, the *a* and *b* parameters show some discontinuity in the close vicinity of the spin transition while the *c* parameter changes continuously.

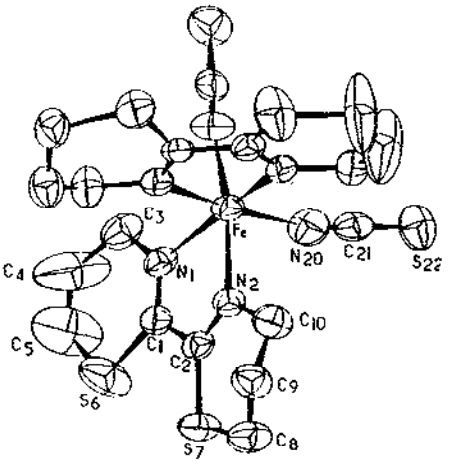

Crystal structure of (**78**).

A ferrous fluorenone thiosemicarbazone (FTsH, (**79**)) complex has been synthesized through the reaction of the ligand with Fe(II)SO4 in ethanol. Based on IR spectroscopic evidence, the complex is formulated as the water-bridged dimer [{Fe(FTsH)(OH$_2$)$_2$}$_2$] · 2SO$_4$ in which the ligands binds in its thioketo form [93].

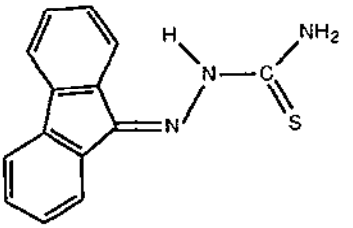

(79)

Ferric complexes of the 3-acetylisoquinoline thiosemicarbazones HL (**80**) and HL' (**81**) have been prepared and examined for antifungal properties. While the octahedral cationic complexes $[FeL_2]FeCl_4$, $[FeL'_2]FeCl_4$ and $[FeL_2]NO_3 \cdot H_2O$, show some antifungal properties, they are not as efficient as the analogous 2-acetylpyridine complexes [94].

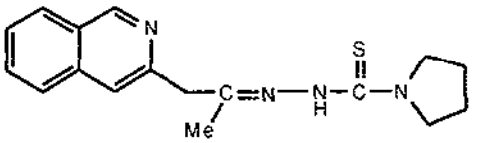

HL

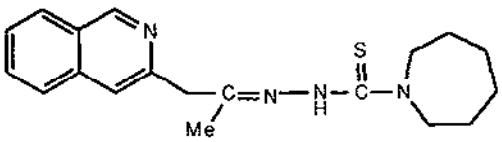

HL'

(**80**), top; (**81**), bottom

The complex tris(5-phenyl-1,3,4-oxadiazol-2-yl)-*N*-benzoyldithiocarbamate)iron(III) has been synthesized and examined for its fungicidal properties [95]. The fungicidal activity at relatively high concentrations (1000 ppm) was found to be 70-80 % of the commmercial fungicide Dithane 45.

Ferrous complexes of the type [Fe(L)(2,2'-bis{(2-mercaptophenyl-thio)diethylamine}] (L = N_2H_4 in complex (**82**), MeOH (**83**), THF (**84**), pyridine (**85**), NH_3 (**86**), $NHCH_3NH_2$ (**87**), $P(OMe)_3$ (**88**) and $P(OPh)_3$ (**89**)) have been synthesized [96]. Donor ligands (N_2H_4 or NH_3) cause high-spin states; σ-donor, π-acceptor ligands (CO, NO, or N_2H_2) cause low-spin states of the Fe centres. The high-spin 18 electron complexes (L = N_2H_4, NH_3, MeOH) exhibit considerably larger Fe-S and Fe-N distances than the low spin 19 electron compounds (L = CO, $^1/_2(N_2H_2)$). The 19 electron complex [Fe(NO)('NHS_4')] with low-spin Fe(II) takes an intermediate position. The ability of the Fe('NHS_4') to bind either hard σ or soft σ/π ligands supports that the fragment is electrochemically as well as chemically flexible. With regard to the reactive centres of Fe-only

nitrogenases, [Fe('NHS_4')] complexes provide a model. Interrelation of Fe spin states, coordination of either σ or σ/π ligands, and substitution lability or inertness support the reduction steps leading from N_2 *via* N_2H_2 over N_2H_4 to NH_3 and enable the final step in a catalytic cycle, the substitution of NH_3 by N_2.

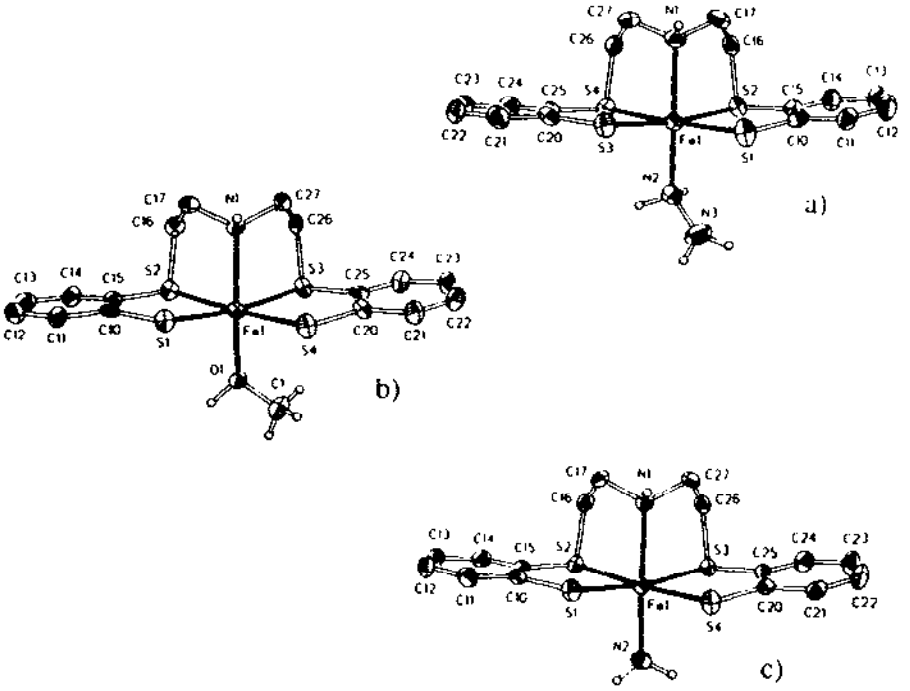

Molecular structures of **82** (a), **83** (b) and **86** (c).
Reprinted with permission from [96]. Copyright 1992 American Chemical Society.

3.9.3 Complexes with other mixed-donor ligands

Ferric complexes of chiral hydroxypyridinethionate, *viz.* tris(*N*-(1-oxo-22(1H)-pyridinethione-6-carbonyl)-R-(+)-1-methylbenzylamine)iron(III) [(**90**)Fe(III)], tris(N-(1-oxo-22(1H)-pyridinethione-6-carbonyl)-S-(-)-1methylbenzylamine)iron(III) [(**91**)Fe(III)] and tris(N-(1-oxo-22(1H)-pyridinethione-6-carbonyl)-1R, 2S-(-)-ephedrine)iron(III) [(**92**)Fe(III)], have been prepared [97]. Based on electronic and CD spectra, the configurations of the complexes are assigned as Λ, Δ and Λ, respectively.

The complexes $[Fe(dtc)_{3-x}L_x]$ (HL = acetylacetone, 8-hydroxyquinoline, glycine, phenylalanine, thiomalic acid; Hdtc = HS_2CNEt_2; x = 1, 2) and $[Fe(dtc)_{3-x}L_x]^+$ (L = phen) have been synthesized and characterized. Magnetic moments of the complexes are at 3.74 – 5.78 μ_B, suggesting a spin crossover equilibrium [98].

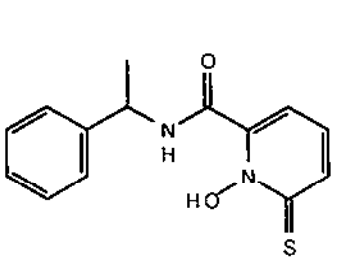

(90), (91)

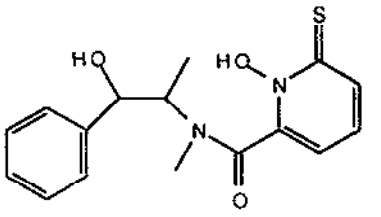

(92)

3.10 *IRON-OXO CLUSTERS*

3.10.1 *Di- and tri-nuclear iron-oxo clusters*

Inelastic neutron scattering spectroscopy indicates that intermolecular exchange coupling takes place in the mixed-valence complex $(Fe_2FeO(O_2CCD_3)_6(C_5D_5N)_5)(C_5D_5N)$. Several transitions can be seen in the energy-transfer range 2-25 cm^{-1}. It is proposed that at low temperatures, a phase consisting of molecules with "frozen" electronic configurations exists and that exchange takes place *via* the electrons of the aromatic rings of interleaved pyridines whereas at higher temperatures, intramolecular $Fe^{2+} \rightarrow Fe^{3+}$ electron transfer takes place [99].

A cluster with a linear iron-oxo core has been synthesized through the reaction of tris(1,4-dimethylimidazol-2-yl)phosphine (T1,4DMIP) with $Fe(ClO_4)_3 \cdot 6H_2O$ and $NaOAc \cdot 3H_2O$ in water; this yields $[Fe_3(\mu\text{-}OH)_2(\mu\text{-}OAc)_4(T1,4DMIP)_2](PF_6)_3$ (**93**). The acetate bridges may be exchanged through reaction with benzoic acid. The crystal structure of the benzoate compound (**94**) has been determined. The EPR spectrum of this compound is consistent with an $S = {}^5/_2$ ground state, suggested to be due to antiferromagnetic coupling between adjacent $S = {}^5/_2$ iron centres [100].

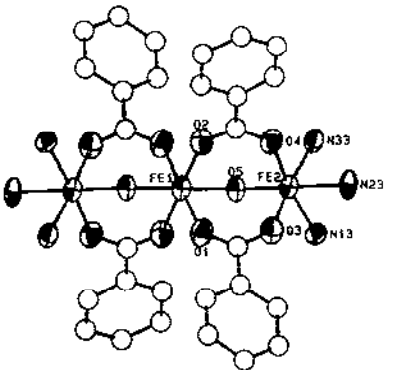

Crystal structure of (**94**).
Reprinted with permission from [100]. Copyright 1992 American Chemical Society.

The reaction of the monomeric ferrous complex [Fe(OBz){HB(3,5-^{i}Pr$_2$pz)$_3$}] with aqueous NaOH affords the bis(μ-hydroxo) complex [Fe{HB(3,5-^{i}Pr$_2$pz)$_3$}]$_2$(OH)$_2$ (**95**) whose structure has been determined by X-ray crystallography [101]. The reaction of this diferrous complex with benzoic acid affords [Fe{HB(3,5-^{i}Pr$_2$pz}$_3$)]$_2$(OH)(OBz) (**96**) quantitatively.

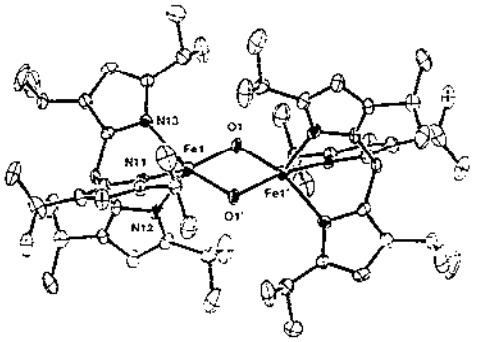

Molecular structure of (**95**).
Reprinted with permission from [101]. Copyright 1992 American Chemical Society.

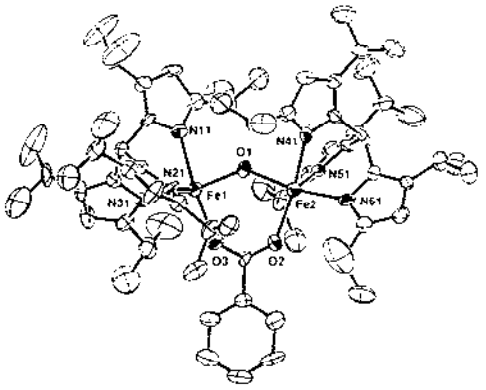

Molecular structure of (**96**).
Reprinted with permission from [101]. Copyright 1992 American Chemical Society.

Reaction of Fe(OAc)$_2$ with the didentate *N*-donor ligand BIPhMe (bis(1-methylimidazol-2-yl)phenylmethoxymethane) (**97**) affords [Fe$_3$(OAc)$_6$(BIPhMe)$_2$] (**98**) whose structure has been determined by X-ray crystallography [102]. The complex adopts a novel linear structure, with one monodentate and two didentate bridging carboxylates spanning each pair of metal atoms. The availability of several different crystal forms of the analogous manganese compound indicates that there are two geometric isomers which are designated *syn* or *anti* depending upon the orientation of the didentate *N*-donor ligands. Temperature-dependent magnetic susceptibility studies revealed ferromagnetic interaction (J ≈ 5±10) between the three iron centres. The [Fe$_3$(OAc)$_6$(BIPhMe)$_2$]

complex is quite stable – attempts to coordinate halides or imidazole to the coordination sites of the terminal metal atoms yielded only starting material.

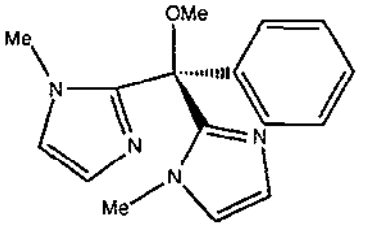

(97)

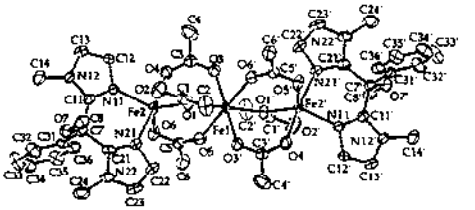

Molecular structure of (98).
Reprinted with permission from [102]. Copyright 1992 American Chemical Society.

Several dinuclear carboxylate-bridged iron-oxo bpy and phen complexes have been synthesized. Reaction of $Fe(ClO_4)_3 \cdot 9H_2O$ with $Na(O_2CR)$ (R = Me, Ph) in the presence of $NaClO_4$ in water or MeOH affords $[Fe_2O(O_2CR)_nB_2(L)_2](ClO_4)_2$ (B = bpy or phen; n = 2, R = Me, L = H_2O; n = 2, R = Ph, L = MeOH; n = 1, R = Ph, L = B). These compounds tend to dimerize to form the corresponding tetranuclear $Fe_4O_2(O_2CR)_7B_2$ complexes. The coupling may be prevented by using an excess of the monodentate ligand (L) [103]. The analogous chloroacetate/bpy and acetate/BIPhMe complexes, $[Fe_2O(O_2CH_2Cl)_2(OH_2)_2(bpy)_2]$ and $[Fe_2O(O_2CH_3)_2(OH_2)_2(BIPhMe)_2]$ have also been synthesized [104]. Magnetic measurements indicate that the iron atoms are antiferromagnetically coupled in both complexes ($J = -113$ cm^{-1} (bpy) and -126 cm^{-1} (BIPhMe)). The former of these two complexes is formed in the reaction of $[Fe_3O(O_2CH_2Cl)_6(H_2O)_3](NO_3)$ with $Fe(NO_3)_3$ and bipyridine in acetonitrile. This complex may also be prepared by the reaction of an acetonitrile solution of $[Fe_2O(NO_3)_4(bpy)_2]$ with an excess of chloroacetic acid. Each iron in $[Fe_2O(NO_3)_4(bpy)_2]$ is coordinated by two didentate nitrate ions and is thus seven-coordinate.

The intramolecular electron transfer of valence-trapped μ-phenoxo-bis(μ-carboxylato)-bridged Fe(II)Fe(III) bimp complexes (Hbimp = (99)) has been studied by ^1H NMR, UV-VIS and

EPR spectroscopies as well as magnetic susceptibility and cyclic voltammetry [105]. The complexes $[Fe(II)Fe(III)(bimp)(O_2CR)_2](X)_2$ (R = Me, Et, Ph; X = ClO_4^-, BF_4^- or BPh_4^-) are strongly paramagnetic and exhibit isotropically shifted ^1H NMR spectra whose ligand resonances indicate an averaged environment, consistent with rapid intramolecular electron transfer on the NMR spectroscopic time scale. All complexes exhibit a broad and relatively weak near-IR absorption band near 1300 nm; this band is assigned as an intervalence transfer band. Fitting of the magnetic susceptibility data for two complexes indicated weak antiferromagnetic interactions ($J \approx -3\ cm^{-1}$), and hence an $S = {}^1/_2$ ground state. Fitting of variable temperature Mössbauer spectra show that valence detrapping occurs as the temperature is increased.

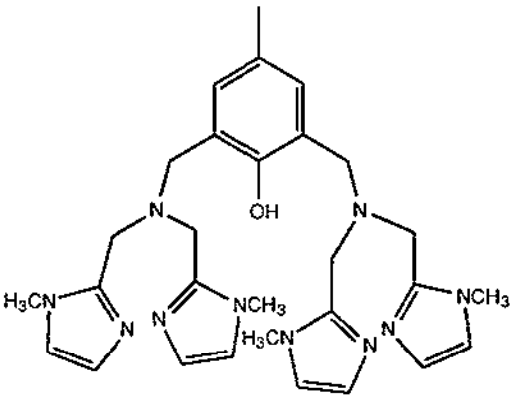

(99)

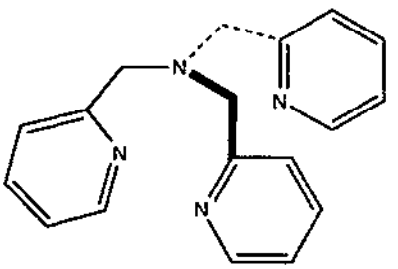

(100)

The dinuclear iron complex $[Fe_2(OAc)_2(TPA)_2](BPh_4)_2$ (TPA = tris(2-pyridylmethyl)amine, **(100)** serves as a model for the diferrous core of ribonucleotide reductase. The crystal structure of the complex reveals that the acetates coordinate to the two Fe(II) centres in a *syn-anti* mode [106]. Variable-temperature magnetic measurements indicate that the carboxylate ligands mediate a weak antiferromagnetic interaction between the metal centres ($J \approx -1\ cm^{-1}$). The NMR spectrum of the complex reveals an averaged environment of the TPA ligand, suggesting a dissociation equilibrium of the dimer. This is further corroborated by a broad signal at $g \approx 9.3$,

which indicates the presence of uncoupled Fe(II) species. Exposure of $[Fe_2(OAc)_2(TPA)_2](BPh_4)_2$ to O_2 results in an immediate reaction forming $[Fe_2O(OAc)_2(TPA)_2](BPh_4)_2$, a (μ-oxo)diferric TPA complex with terminal monodentate acetates, which in turn converts readily to the previously characterized $[Fe_2O(OAc)_2(TPA)_2]^{3+}$ complex in the presence of protic solvents.

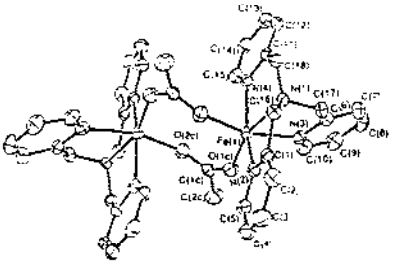

Crystal structure of $[Fe_2(OAc)_2(\mathbf{100})_2](BPh_4)_2$.

Ab initio Hartree-Fock calculations have been used to investigate the angular and distance dependence of the magnetic coupling in $Na_2[Fe_2OCl_6]$. The results indicate that the magnetic interaction is quite dependent on the Fe-O distance; the coupling constant varies from approximately 210 cm^{-1} to 140 cm^{-1} as the Fe-O distance increases from 1.65 to 1.95 Å [107].

Addition of nitrilotriacetic acid (H_3nta) and NaOH to an aqueous $FeCl_3$ solution results in the formation of the oxo-bridged complex $[\{Fe(nta)(H_2O)\}_2O]^{2-}$ which, in the pH range 5–5.5, may be precipitated as the barium salt through addition of $BaCl_2$. The molecular structure has been determined [108].

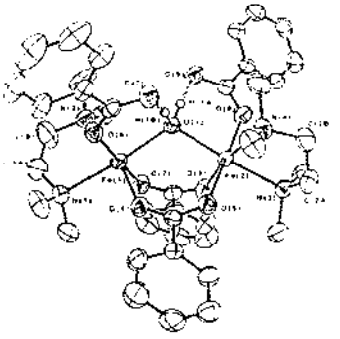

Crystal structure of (**101**).

The first μ-aqua-bridged diiron(II) complex, $Fe_2(H_2O)(O_2CR)_4(tmen)_2$ (**101**) has been prepared by the reaction of $Fe(O_2CMe)_2 \cdot 4H_2O$ with 1 equivalent of tmen in acetonitrile [109]. The analogous benzoate compound can be prepared from a mixture of $Fe(CF_3SO_3)_2 \cdot CH_3CN$, $PhCO_2H$, Et_3N and H_2O in acetonitrile. The Fe-Fe (3.05Å) and Fe(μ-O) distances (2.18 Å) are

considerably larger than similar diferrous hydroxide-bridged compounds. The ^{1}H NMR spectrum of the acetate compound is consistent with ligand fluxionality or possibly a dissociation equilibrium; the benzoate complex appears to dissociate in protic or strongly coordinating solvents.

Hemerythrin models have been synthesized by the "self-assembly" method through the reaction of $Fe(ClO_4)_3 \cdot 9H_2O$ with bis((1-methylimidazole-2-yl)methyl)amine (bmima, (**102**)), NEt_3 and benzoic or acetic acid. Recrystallization from MeCN affords the complexes $[Fe_2O(bmima)_2(O_2CR)_2](ClO_4)_2 \cdot 2MeCN \cdot xH_2O$ (R = Ph, x = 2; R = Me, x = 0, 1.5). The crystal structure of $[Fe_2O(bmima)_2(O_2CPh)_2](ClO_4)_2 \cdot 2MeCN \cdot H_2O$ (**103**) is shown. Magnetic susceptibility data indicate that the J-values of the hydrated species are temperature-dependent, probably due to hydrogen-bonding of the solvate to the oxo-bridges [110].

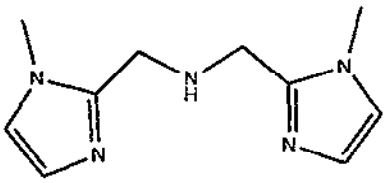

(**102**)

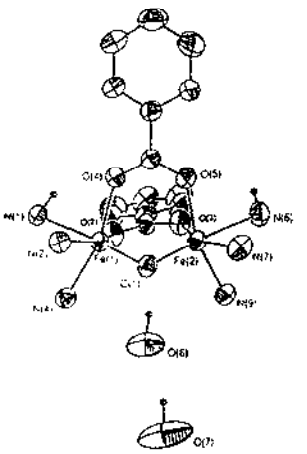

Crystal structure of (**103**).
Reprinted with permission from [110].
Copyright 1992 American Chemical Society.

Reaction of $Fe(NO_3)_3 \cdot 9H_2O$ with *N,N,N',N'*-tetrakis(2-pyridylmethyl)-2-hydroxy-1,3-diaminopropane [H(HPTP), (**104**)] and NEt_3 forms $[Fe_2(HPTP)(OH)(NO_3)_2](ClO_4)_2$. Magnetic susceptibility data indicate a ferromagnetic coupling constant J of –23.9 cm^{-1}. The complex forms an unstable violet adduct with hydrogen peroxide in water. The instability of the complex is suggested to be due to catalase-like activity of the iron-oxo cluster. Bleomycin-like activity is also found; the complex is able to degradate DNA in the presence of H_2O_2 [111].

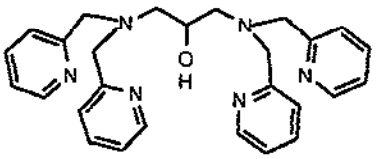

(**104**)

The dinuclear iron (III) compounds $[Fe_2(HPTB)(OH)(NO_3)_4]^+$, $[Fe_2(pac)(OAc)]^{2-}$ and $[Fe_2(HPTP)(OH)(NO_3)_2](ClO_4)_2$ (HPTB = *N,N,N',N'*-tetrakis(2-benzimidazolmethyl)-2-hydroxy-1,3-diaminopropane, (**105**), H_5pac = *N,N'*-(2-hydroxy-5-methyl-1,3-xylylene)bis(*N*-carboxymethyl glycine), (**106**) have been reacted with the spin-trapping reagent DMPO (5,5-dimethyl-3,4-dihydropyrrole *N*-oxide). The observed EPR spectra are consistent with the formation of DMPO-OH. It is suggested that the dinuclear complexes activate oxygen (*via* a peroxide adduct) and that DMPO reacts with the activated complex to form the hydroxo derivative. The formation of DMPO-OH may thus be formed without the presence of OH· radicals [112].

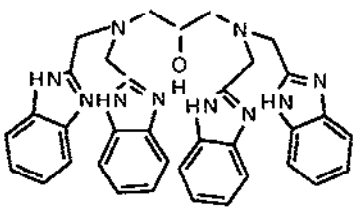

(**105**)

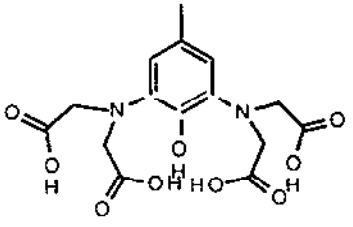

(**106**)

The reaction of $[NEt_4]_2[Fe_2OCl_6]$ with 3,5-di-tertbutylcatechol (DTBC) in MeCN affords the dinuclear complex $[NEt_4]_2[Fe_2OCl_4(dtbc)_2]\cdot MeCN$. This compound, as well as $[NEt_4]_2[Fe_2OCl_6]$ and $FeCl_3$ have been used as catalysts for hydroxylation reactions. Substrates used include methane ethane, n-hexane, cyclohexane and adamantane [113]. Reductants used were hydroquinone, hydrozobenzene, and phenylhydrazine. Kinetic isotope effects and reactivity patterns of substrates suggest that an Fe(IV)-O-Fe(IV)=O species is the active catalyst. The dinuclear complexes are approximately 10 times more effective than $FeCl_3$. Maximum efficiency and alchohol selectivity are achieved with the $[NEt_4]_2[Fe_2OCl_4(dtbc)_2]\cdot MeCN$-phenylhydrazine system.

Treatment of the "synthon" $[NEt_4]_2[Fe_2OCl_6]$ with NaOBz or NaOAc and [2-(2-pyridyl)ethyl](2-pyridyl)ethyl](2-pyridylmethyl)amine (**107**) or methyl[2-(2-pyridyl)ethyl](2-pyridylmethyl)amine (**108**) in MeCN affords the complexes $[Fe_2(\mu\text{-}O)(\mu\text{-}X)_2L_2]^{2+}$ (X = OBz, L = (**107**); X = OAc; L = (**108**)) [114]. The analogous complex $[Fe_2(\mu\text{-}O)(\mu\text{-}(PhO)_2PO_2)_2(\mathbf{108})_2]$ was prepared by deprotonation of $(PhO)_2PO_2$ in the presence of $[NEt_4]_2[Fe_2OCl_6]$ and (**108**). It may also be obtained by exchange with labile acetate groups of $[Fe_2(\mu\text{-}O)(\mu\text{-}X)_2(\mathbf{108})_2]^{2+}$. It is

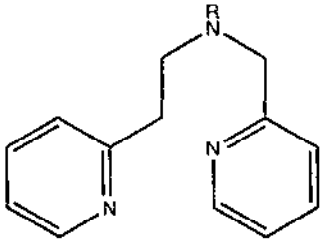

(**107**) (R = H), (**108**) (R = Me)

suggested that unsymmetrical ligands increases the asymmetry of the complexes and thus contribute to a stronger magnetic coupling pathway, as evidenced by the strong antiferromagnetic coupling in these complexes (J = –127 (BzO^-), –125 (AcO^-) and –108 cm^{-1} (Ph_2PO^{4-})).

3.10.2 Heterometallic iron-oxo clusters

The synthesis of several asymmetric homo-and heterodinuclear complexes of the type $[LM^1(\mu\text{-}O)(\mu\text{-}CH_3CO_2)_2M^2L']^{2+}$ (M^1, M^2 = Fe(III), Mn(III), Cr(III); L = tacn, L' = Me_3tacn) has been achieved by the cohydrolysis of (tacn)MCl_3 complexes in MeOH solutions which contain an excess of NaOAc. The following complexes have been synthesized: $M^1 = M^2$ = Fe(III); M^1 = Mn(III), M^2 = Fe(III); M^1 = Fe(III), M^2 = Mn(III); M^1 = Fe(III), M^2 = Ru(III) and M^1 = Cr(III), M^2 = Fe(III) [115, 116]. The crystal structures of the perchlorate salt of the FeMn dimer (**109**) as well as hexafluorophosphate salt of the CrFe dimer (**110**) have been determined. All complexes were found to be antiferromagnetically coupled. The FeRu species may be oxidized with $Na_2S_2O_8$ in H_2O to form the corresponding trianion. Both the FeRu and CrFe species may be protonated. In the latter case, this decreases the antiferromagnetic coupling and is rationalized by the lengthening of the M-O bonds. A general theoretical treatment of magnetic coupling in complexes containing the μ-oxo-bis(μ-acetato) dimetal cores is presented together with supporting theoretical calculations [116].

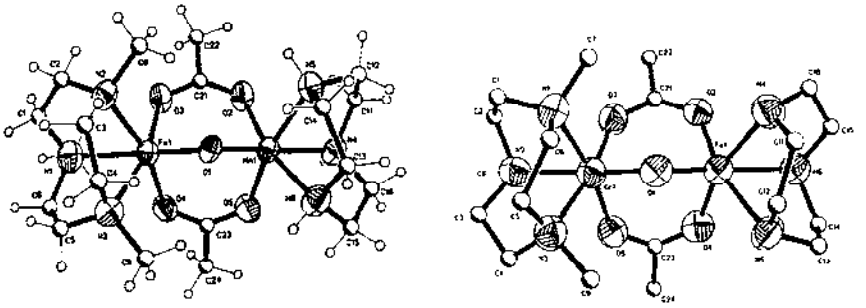

Crystal structures of (**109**) (left) and (**110**) (right).

The redox reaction between *trans*-dioxotetraphenylporphyrin Ru(IV) and two equivalents of Fe(II) salicylideneamine results in the transfer of two electrons and the formation of the bis-μ-oxo trimetallic complex [Ru(IV)(tpp){OFe(III)(salmah)}$_2$] (salmah = dianion of *N,N'*-4-methyl-4-azaheptane-1,7-diylbis(salicylideneamine)). An X-ray structure determination of the complex shows it to be a centrosymmetric species containing a linear Fe-O-Ru-O-Fe unit. The room temperature magnetic moment of the trimetallic complex is slightly lower than the spin only value calculated for an Fe(III)Ru(IV)Fe(III) $d^5d^4d^5$ ($S = {}^5/_2\text{-}1\text{-}{}^5/_2$) system. Variable temperature magnetic measurements give clear evidence of ferromagnetic exchange coupling within the Fe(III)-O-Ru(IV)-O-Fe(III) unit [117].

3.10.3 Polynuclear iron-oxo clusters

The oxide cluster $Na_2Fe_6O(OMe)_{18} \cdot 6$ MeOH (**111**) can be synthesized from the reaction of NaOMe with $FeCl_3$ in methanol. In its idealized O_h geometry, the central oxygen atom is in the centre of the octahedron formed by six iron(III) atoms which are linked to each other by 12 μ_2- methoxide bridges. All 24 of the methyl groups are located on the periphery of the molecule, generating a hydrophobic surface making the compound soluble in non-polar solvents. Poor crystal integrity prevented collection of a complete data set [118].

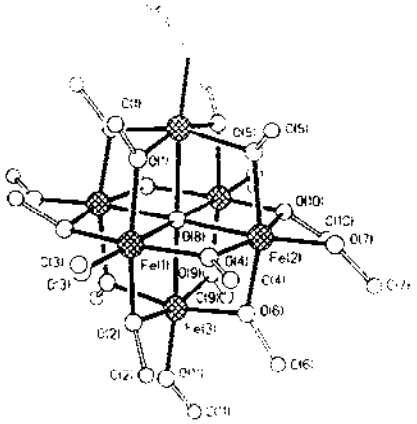

Crystal structure of (**111**).

The tetracation $[Fe_3O_2(OH)(tren)_3]^{4+}$ disproportionates to $[Fe_6O_2(OMe)_{12}(tren)_2]^{2+}$ (**112**) in methanol [119]. The latter compound may also be synthesized through the exposure of a methanol solution of $Fe_3(CF_3SO_3)_2 \cdot$ MeCN to air. The crystal structure of (**112**) is shown. Each iron is six-coordinate — there are two μ_4-O^{2-} ions. Mössbauer spectra are consistent with high-spin Fe(III) and three distinguishable sites — corresponding to the three crystallographically distinct sites — are found in high-field spectra. It is suggested that the room-temperature ground state is formed by two ferromagnetically coupled $S = {}^5/_2$ states, *i.e.* $S = 5$.

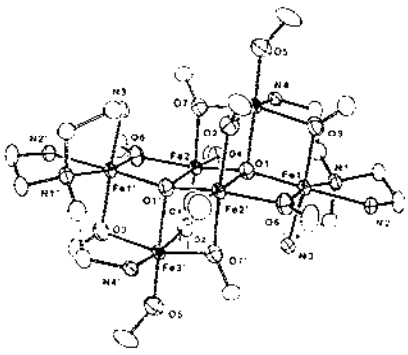

Crystal structure of (**112**).

Depending on the stoichiometry, the reaction of $Fe(NO_3)_3 \cdot 9H_2O$ with the ligand heidi [H_3heidi = $N(CH_2CO_2H)_2(CH_2CH_2OH)$] yields the clusters $[Fe(heidi)(H_2O)]_2$ (**113**), $[Fe_{19}(\mu_3\text{-}O)_6(\mu_3\text{-}OH)_6(\mu_2\text{-}OH)_8(heidi)_{10}(H_2O)_{12}]$ and $[Fe_{17}(\mu_3\text{-}O)_4(\mu_3\text{-}OH)_6(\mu_2\text{-}OH)_{10}(heidi)_8(H_2O)_{12}](NO_3)_4 \cdot 6\ H_2O$ [120]. The latter two clusters consist of the $[Fe_7(\mu_3\text{-}OH)_6(\mu_2\text{-}OH)_4(\{\mu_3\text{-}O)Fe\}_2]^{13+}$ core (**114**) which is enclosed in a shell of ligands which are complexed to further iron atoms.

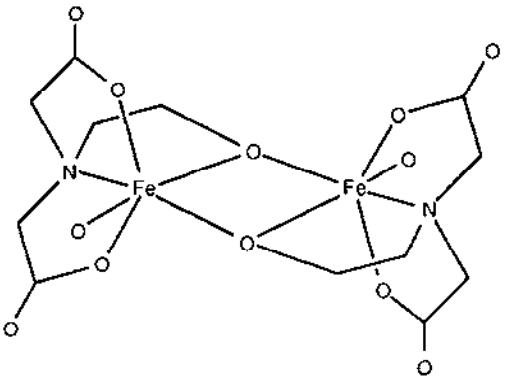

(**113**)

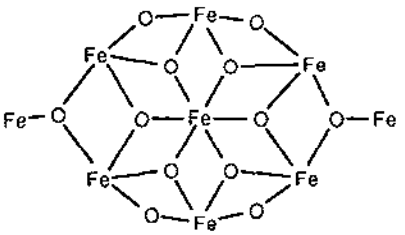

(**114**)

3.11 IRON-SULFUR, SELENIUM AND TELLURIUM CLUSTERS

3.11.1 Iron-sulfur cubanes

The reaction of $[Fe(MeCp)(CO)_2]_2$ with an excess of sulfur in refluxing toluene produces $[Fe_4S_4(MeCp)_4]^{0-2+}$ and $[Fe_4S_5(MeCp)_4]^{0-2+}$; the cations have been isolated as PF_6^- salts [121]. The Fe_4S_5 clusters contain S_2-units which replace one of the μ_3-sulfurs in a regular Fe_4S_4 cubane. The S_2 moiety bridges three iron atoms — one sulfur coordinates to two iron atoms and the other sulfur coordinates to a third atom. Proton NMR indicates that the S_2 moiety is fluxional. The crystal structure of $[Fe_4S_5(MeCp)_4]^+$ (**115**) has been determined; a schematic depiction of the iron-sulfur core is shown below.

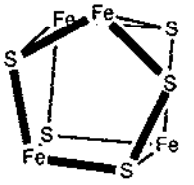

(115)

The oxidation of $[Fe_4S_4(S\text{-}2,4,6\text{-}(^iPr)_3C_6H_2)_4]^{2-}$ by $[Fe(CN)_6]^{3-}$, Ag^+, I_2, CPh_3^+ in CH_2Cl_2 or MeCN results in a one-electron metal-based oxidation to form the HiPIP analog $[4Fe\text{-}4S]^{3+}$ cubane cluster. Use of the same oxidants in an aqueous medium (DMF/H_2O or MeCN/H_2O) results in a 2-electron oxidation and subsequent cluster breakdown to form a short-lived $[3Fe\text{-}4S]^+$ centre as evidenced by EPR spectroscopy [122].

The cubane-like iron-sulfur clusters $[(C_5Me_5)_3(Ph_2C_2S_2)Fe_4S_5]^n$ (n = 0, +1) have been synthesized by thermolysis of $[(Cp')_2Fe_2(CO)_4]$ in the presence of phenylacetylene and S_8 [123]. The crystal structure of the neutral cluster (**116**) is shown. The cluster contains one FeS_2C_2 metallacycle which has been previously observed in a related Fe_4S_4 cluster.

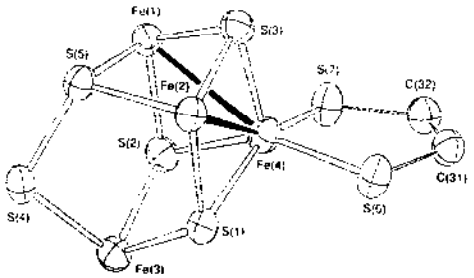

Crystal structure of (**116**).
Reprinted with permission from [123]. Copyright 1992 American Chemical Society.

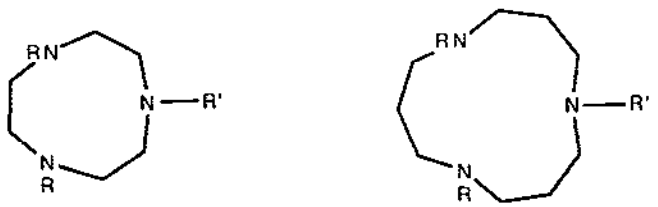

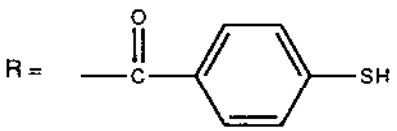

(**117**), left, and (**118**), right.

Two tripodal ligands based on substitution on the nitrogen atom of tacn and 1,5,9-triazacyclododecane have been synthesized; they are 1,4,7-tris(4-mercaptobenzoyl)-1,4,7-triazacyclononane (**117**) and 1,5,9-tris(4-mercaptobenzoyl)-1,5,9-triazacyclododecane (**118**). These ligands have been coordinated to $[Fe_4S_4(SR)_4]^{2-}$ clusters (R = Et, Bu) to form the site-differentiated clusters $[Fe_4S_4(L)(SR)]^{2-}$ [124].

The reduction of $Fe_2(SR)_2(NO)_4$ by Na, KH or $M(BR_3H)$ (M = Li, R = Et; M = Li, K, R = Bu) in thf is reported to form $[Fe_2(SR)_2(NO)_4]^{2-}$ [125]. The formation of the product as the dianion is based on the conductivity of the potassium salt in methanol solution. However, based on the spectroscopic similarities of this compound with that of an earlier report, Glidewell and Lambert [126] argue that the product is the monoanion $[Fe_2(SR)_2(NO)_4]^-$.

The cubane-like $[Fe_4Te_4(PEt_3)_4]PF_6$ and the stellated octahedron $[Fe_6Se_8(PEt_3)_6]PF_6$ have been synthesized by the reaction of $Fe(ClO_4)_2$ with PEt_3 and H_2X (X = Te, Se) in the presence of PF_6^-. Room temperature solid state magnetic susceptibilities have been measured using a Faraday balance; the calculated magnetic moments are 6.8 and 7.8 μ_B for Fe_4Te_4 and Fe_6Se_8, respectively. X-ray structure determination reveals the Fe_4Te_4 cluster (**119**) displays cubane-like geometry [127].

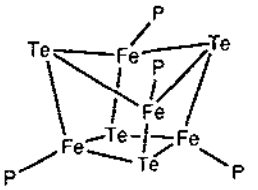

(**119**)

Previously it was thought that the formation of $[Fe_4S_3(NO)_7]^-$ was necessary for the synthesis of $[Fe_2SR_2(NO)_4]$. The reaction of various Fe(II) salts with sodium nitrate with methionine yields direct formation of $[Fe_2(SMe)_2(NO)_4]$. Control experiments using iron chloride instead of iron sulfate determined the sulfur is derived from methionine rather than the reduction of sulfate. The complex $[Fe_2(SMe)_2(NO)_4]$ is also produced when $[Fe_4S_3(NO)_7]^-$ reacts with methionine although the source of the sulfur is not known [128]. Reaction of $Fe(SO_4) \cdot 7H_2O$ with sodium nitrite, sodium ascorbate and a sulfur source (various sulfur-containing amino-acid derivatives based on cysteine and methionine) under elevated temperature (autoclavation or microwave exposure) yielded the new compounds $[Fe_2(SR)_2(NO)_4]$ (R = $CH_2(NH_2)COOEt$, $CH_2CH(NHCOMe)COOH$, $CMe_2CH(NH_2)COOH$, $CMe_2CH(NHCOMe)COOH$ as well as some $Na[Fe_4S_3(NO)_7]$, as evidenced by IR, ^1H and ^{13}C NMR spectroscopy and mass spectrometry [129].

3.11.2 Heterometallic iron-sulfur clusters

Coucouvanis *et al.* report the synthesis and characterization of the cubane $[M(CO)_3Fe_3S_4L_3]^{3-}$ (M = Mo, W and L = Cl, SEt, SBz, OPh, and SC_6H_4-*p*-OMe) clusters containing $[MFe_3S_4]^0$ cores as analogues to the reduced three-iron centres in ferredoxins [130].

X-ray diffraction measurements on $[Et_4N]_3[Fe_3S_4(SEt)_3Mo(CO)_3 \cdot MeCN$ (**120**) show that the $Mo(CO)_3$ fragment interacts weakly with the Fe_3S_4 ligand. The Fe_3S_4 exhibits hyperfine parameters similar to those reported for the Fe_3S_4 centres of the iron-sulfur proteins of *A. vinelandii Fd II* and *D. gigas*. Oxidative decarbonylation reactions of $[Et_4N]_3[Fe_3S_4(L)_3Mo(CO)_3]$ with quinone affords the solvated single cubane $[Et_4N]_2[Fe_3S_4(Cl)_3Mo(MeCN)(cat)]$ when the terminal ligand on the iron site is Cl^- and the doubly-bridged double cubane $[Et_4N]_4[Fe_3S_4(SEt)_3Mo(cat)_2$ when the terminal ligand is EtS^-. Upon heating in solution the $[Et_4N]_3[Fe_3S_4(L)_3Mo(CO)_3]$ cluster (L = Cl^-, *p*-$COMePhO^-$) are converted to the corresponding prismane-adduct, octanuclear clusters $(Et_4N)_4[Fe_6S_6(L)_9\{Mo(CO)_3\}_2]$.

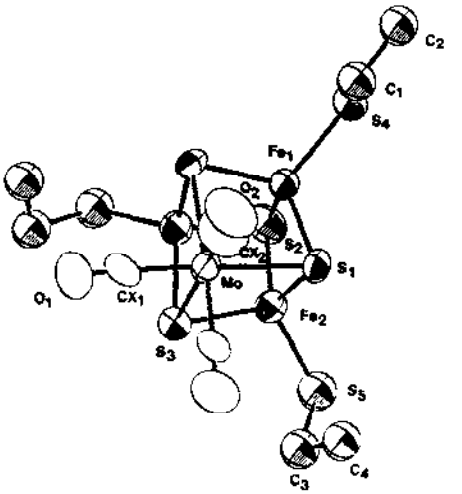

Crystal structure of (**120**).
Reprinted with permission from [130]. Copyright 1992 American Chemical Society.

The reaction of the linear $[Fe_3Q_4(SEt)_4]^{3-}$ (Q = S, Se) with $Ni(PPh_3)_4$ in MeCN solution affords $[NiFe_3Q_4(PPh_3)(SEt)_3]^{2-}$ (**121**) and $[NiFe_3Q_4(SEt)_4]^{3-}$. The reactions involve reductive rearrangement of the linear Fe3-cluster to a cuboidal fragment and capture of the nickel atom. The $(Et_4N)^+$ salt of $[NiFe_3Q_4(SEt)_4]^{3-}$ (Q = Se) contains an M_4S_4 cubane unit but with disordered Ni and Fe subsites. The structural, magnetic, and spectroscopic results are consistent with the charge distribution $[Fe_3Q_4]^{1-}$ ($S = {}^5/_2$) + Ni^{2+} ($S = 1$). Antiparallel coupling of the two fragment spins yield an $S = {}^3/_2$ ground state. This spin coupling causes oppositely signed isotropic NMR shifts of the identical ligands at Ni and Fe subsites. The cluster (**121**) (Q = S) undergoes regiospecific substitution at the Ni subsite when reacted with phosphines, CN^-, and isonitrile. The synthetic clusters have been found to be isoelectronic with the reconstituted $NiFe_3S_4$ species formed with the *P. furiosus* ferredoxin; they also have the same ground state as the biological cluster [131].

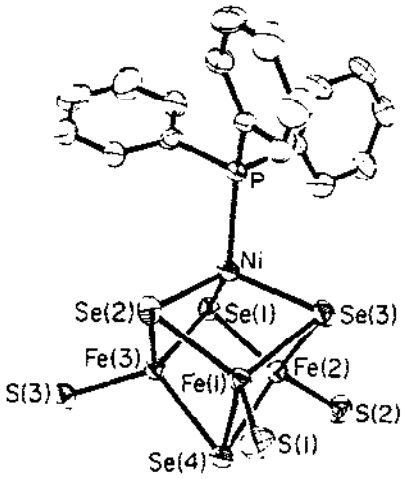

Crystal structure of (**121**) (Q = Se).
Reprinted with permission from [131]. Copyright 1992 American Chemical Society.

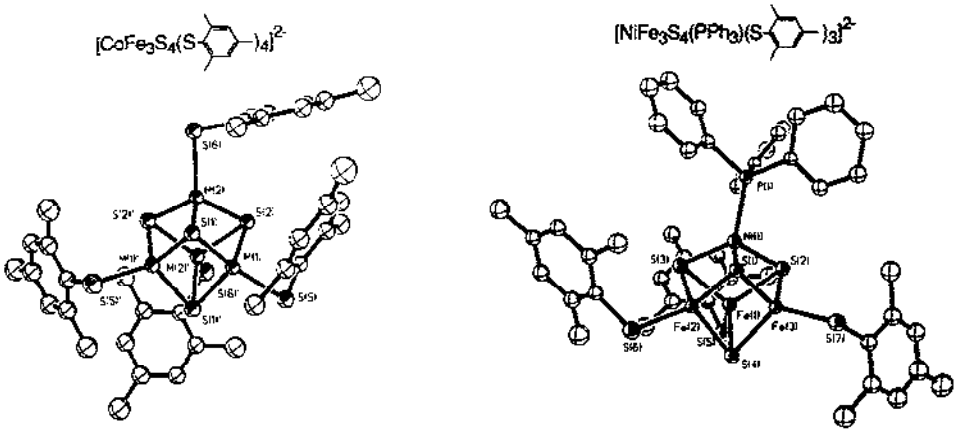

Crystal structures of (**122**) (left) and (**123**) (right).
Reprinted with permission from [132]. Copyright 1992 American Chemical Society.

Similarly, the heterometal cubane-type clusters $[CoFe_3S_4(SMes)_4]^{2-}$ (**122**), (HSMes = mesitylthiol) and $[NiFe_3S_4(PPh_3)(SMes)_3]^{2-}$ (**123**) have been prepared as Et_4N^+ salts by reductive rearrangement reactions of the linear cluster $[Fe_3S_4(SMes)_4]^{3-}$ with Co(I) and Ni(0) complexes. In (**122**), the Fe subsites appear to be more reactive to ligand substitution by thiol than is the Co subsite. The three-member electron transfer series $[CoFe_3S_4]^{3+/2+/1+}$ and $[NiFe_3S_4]^{3+/2+/0}$ have been investigated by cyclic voltammetry. For the reversible couples $[MFe_3S_4(SMes)_4]^{2-/3-}$ the

order of potentials is M = Fe < Co (0.18 V) < Ni (0.30 V), with the indicated potential differences vs. M = Fe. The close correspondence of Mössbauer and EPR parameters of the synthetic clusters (**122**) and (**123**) with those of protein $[CoFe_3S_4]^{2+}$ and $[NiFe_3S_4]^{1+}$ clusters indicates that the latter contain the tightly bound cubane-type structures established by X-ray diffraction for the synthetic species. Mössbauer spectroscopy reveals that (**122**) and the protein-bound $[CoFe_3S_4]^{2+}$ cluster of *D. gigas* ferredoxin II have equivalent electronic structures at 4.2 K. The Mössbauer isomer shifts imply the fragment formulations Co^{2+} ($S = {}^3/_2$) + $[Fe_3S_4]^0$ ($S = 2$) and Ni^{2+} ($S = 1$) + $[Fe_3S_4]^{1-}$ ($S = {}^5/_2$), with antiparallel spin coupling affording the observed $S = {}^1/_2$ and ${}^3/_2$ ground state, respectively [132].

3.11.3 Other iron-sulfur clusters

Changes of reaction conditions in the self assembly of the cyclic cluster $[\alpha\text{-}Na_2Fe_{18}S_{30}]^{8-}$ (**124**) has afforded the synthesis of two new high-nuclearity clusters. The black compounds $(Bu_4N)_6Na_4Fe_{18}S_{30}$ or $(Bu_4N)_{4.5}Na_{13.5}Fe_{20}Se_{38.2} \cdot PhNHCOMe \cdot 12EtOH$ are afforded in good yields from the reaction system $FeCl_3$:3 Na(PhNCOMe):n Li_2Q/EtOH (n = 1.8, Q = S; n = 2, Q = Se) with Bu_4NBr. The compound $(Bu_4N)_6Na_4Fe_{18}S_{30} \cdot 8EtOH$ contains the cluster $[\beta\text{-}Na_2Fe_{18}S_{30}]^{8-}$ (**125**), which is a structural isomer of (**124**). The compound $(Bu_4N)_{4.5}Na_{13.5}Fe_{20}Se_{38.2} \cdot PhNHCOMe \cdot 12EtOH$ contains the bicyclic ellipsoidal cluster $[Na_9Fe_{20}Se_{38}]^{9-}$ (**126**). The structure of the latter cluster is built up from 21 non-planar Fe_2Se_2 rhombs, 15 of which share vertices to form three $Fe_6(\mu_2\text{-}Se)_{10}$ chains. These chains are anchored at each end of the molecule by attachment to three edge-shared bridgehead rhombs. The selenium-rich interior cavity encapsulates nine sodium ions. Both clusters have singlet ground states, are electronically delocalized and antiferromagnetically coupled, and are of dimensions that place them in the nanometer size range [133].

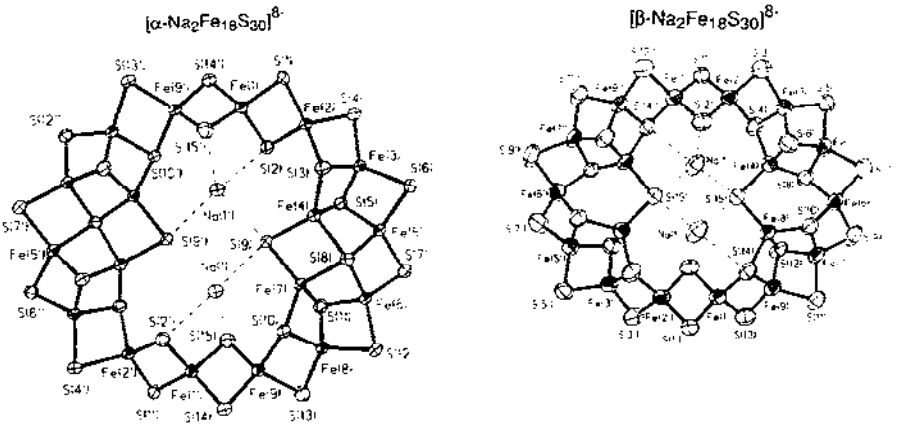

Crystal structure of (**124**) (left) and (**125**) (right).
Reprinted with permission from [133]. Copyright 1992 American Chemical Society.

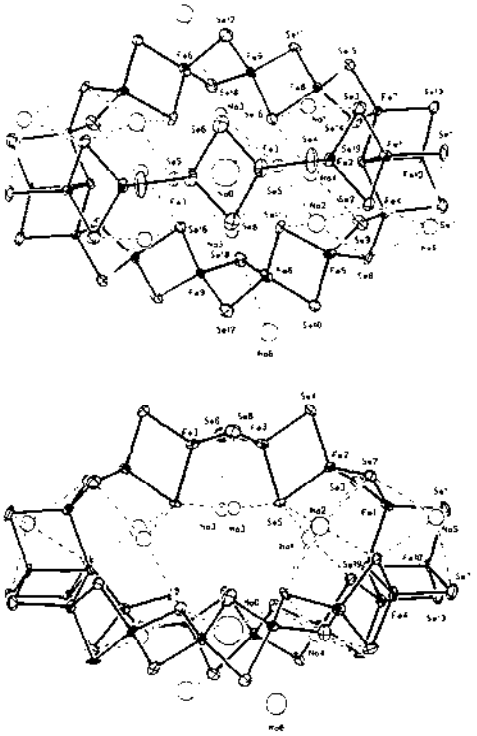

Two views of the molecular structure of (**126**).

ACKNOWLEDGEMENT

The authors wish to thank Prof. Cortlandt G. Pierpont for providing the figures of compounds (**57**) and (**58**).

REFERENCES

1. U. Schubert, S. Gilbert and S. Mock, *Chem. Ber.*, 125 (1992) 835.
2. F. Maseras, M. Duran, A. Lledos and J. Bertran, *J. Am. Chem. Soc.*, 114 (1992) 2922.
3. D. Schroeder, J. Hrusak and H. Schwarz, *Helv. Chim. Acta* 75 (1992) 2215
4. M. M. Korobov, Y. V. Pervova and L. N. Sidorov, *Mendeleev Commun.*, (1992) 41.
5. S. Murahashi, Y. Oda and T. Naota, *J. Am. Chem. Soc.*, 114 (1992) 7913.
6. G. B. Shul'pin and A. N. Druzhinina, *Mendeleev Commun.*, (1992) 36.
7. A. Barrios, M. del Mar, R. Jimenez, E. Munoz, F. Sanchez, M. L. Moya, S. Alshehri and J. Burgess, *Transition Metal Chem. (London)*, 17 (1992) 231.
8. M. E. Pena, J. R. Leis and G. Stedman, *Transition Metal Chem. (London)*, 17 (1992) 123.
9. G. Albertin, S. Antoniutti, E. Del Ministro and E. Bordignon, *J. Chem. Soc., Dalton Trans.*, (1992) 3203.
10. C. Roux, J. Zarembowitch, B. Gallois and M. Bolte, *New. J. Chem.*, 16 (1992) 671.
11. C. K. Cho and A. S. Secco, *Acta Crystallogr., Sect. C*, 48, (1992) 165.
12. E. C. Constable and A. M. W. Cargill Thompson, *J. Chem. Soc., Dalton Trans.*, (1992) 2947.

13. J. D. Crane and J. P. Sauvage, *New J. Chem.*, 16 (1992) 649.
14. S. H. Cho, D. Wang, K. Han and K. Kim, *Inorg. Chem.*, 31 (1992) 519.
15. E. Mulliez, G. Guillot-Edelheit, P. Leduc, J. C. Chottard, C. Bois, A. Bousseksou and W. Nitschke, *New J. Chem.*, 16 (1992) 435.
16. R. E. Shepherd, T. J. Lomis and R. R. Koepsel, *J. Chem. Soc., Chem. Commun.*, (1992) 222.
17. R. W. Saalfrank, O. Struck, K. Nunn, C. J. Lurz, R. Harbig, K. Peters, H. G. Von Schnering, E. Bill and A. X. Trautwein, *Chem. Ber.*, 125 (1992) 2331.
18. M. Bonamico, V. Fares, A. Flamini and N. Poli, *J. Chem. Soc., Dalton Trans.*, (1992) 3273.
19. N. V. Gerbeleu, V. B. Arion, Y. A. Simonov, V. E. Zavodnik, S. S. Stavrov, K. I. Turta, D. I. Gradinaru, M. S. Birca, A. A. Pasynskii and O. Elbert, *Inorg. Chim. Acta*, 202 (1992) 173.
20. T. J. Collins, B. G. Fox, Z. G. Hu, K. L. Kostka, E. Munck, C. E. F. Rickard and L. J. Wright, *J. Am. Chem. Soc.*, 114 (1992) 8724.
21. M. Di Vaira, F. Mani and P. Stoppioni, *J. Chem. Soc., Dalton Trans.*, (1992) 1127.
22. H. S. Mountford, L. O. Spreer, J. W. Otvos, M. Clavin, K. J. Brewer, M. Richter and B. Scott, *Inorg. Chem.*, 31 (1992) 717.
23. J. P. Cornelissen, J. H. van Diemen, L. R. Groeneveld, J. G. Haasnoot, A. L. Spek and J. Reedjik, *Inorg. Chem.*, 31 (1992) 198.
24. S. Ruettimann, C. M. Moreau, A. F. Williams, G. Bernardinelli and A. W. Addison, *Polyhedron*, 11 (1992) 635.
25. C. M. Che, W. H. Leung, C. K. Li, H. Y. Cheng and S. M. Peng, *Inorg. Chim. Acta*, 196 (1992) 43.
26. A. A. El-Samahy, E.-E. A. Abu-Gharib, A.-E. Eltaher, R. M. El-Khatib and J. Burgess, *Transition Metal Chem.* (London), 17 (1992) 438.
27. N. R. S. Kumar and M. Nethaji, *Acta Crystallogr., Sect. C*, 48, (1992) 1105.
28. M. Hanack and R. Grosshans, *Chem. Ber.*, 125 (1992) 1243.
29. M. K. Safo, G. P.Gupta, C. T. Watson, U. Simonis, F. A. Walker and W. R. Scheidt, *J. Am. Chem. Soc.*, 114 (1992) 7066.
30. F. A. Walker, U. Simonis, H. Zhang, J. M. Walker, T. M. Ruscitti, C. Kipp, M. A. Amputch, B. V. Catillo, S. H. Cody, D. L. Wilson, R. E. Gaul, G. J. Yong, K. Tobin, J. T. West and B. A. Barichievich, *New J. Chem.*, 16 (1992) 609.
31. H. Nasri, K. J. Haller, Y. Wang, B. H. Huynk and W. R. Scheidt, *Inorg. Chem.*, 31 (1992) 3459.
32. L. M. Mink, K. A. Christensen and F. A. Walker, *J. Am. Chem. Soc.*, 114 (1992) 6930.
33. L. Leondiadis, M. Momenteau and A. Desbois, *Inorg. Chem.*, 31 (1992) 4691.
34. J. P. Fitzgerald, B. S. Haggerty, A. L. Rheingold and L. May, *Inorg. Chem.*, 31 (1992) 2006.
35. C. T. Brewer and G. Brewer, *J. Chem. Soc., Dalton Trans.*, (1992) 1669.
36. J. Zakrzewski, M. Cesario, J. Guilhelm and C. Giannotti, *J. Chem. Soc., Dalton Trans.*, (1992) 3059.
37. D. Mandon, R. Weiss, K. Jayaraj, A. Gold, J. Terner, E. Bill and A. X. Trautewein, *Inorg. Chem.*, 31 (1992) 4404 .
38. K. Yamaguchi, Y. Watanabe and I. Morishima, *J. Chem. Soc., Chem. Commun.*, (1992) 1721 .
39. H. Fujii and K. Ichikawa, *Inorg. Chem.*, 31 (1992) 1110.
40. K. Yamaguchi, Y. Watanabe and I. Morishima, *J. Chem. Soc., Chem. Commun.*, (1992) 1709.
41. K. Tajima, K. Mikami, K. Tada, S. Oka, K. Ishizu and H. Ohya-Nishiguchi, *Inorg. Chim. Acta*, 194 (1992) 57.
42. I. Artaud, H. Grennberg and D. Mansuy, *J. Chem. Soc., Chem. Commun.*, (1992) 1036.
43. K. R. Rodgers, R. A. Reed, T. G. Spiro and Y. O. Su, *New J. Chem.*, 16 (1992) 533.
44. Y. Adam, J. Bernadou and B. Meunier, *New J. Chem.*, 16 (1992) 525.
45. W. R. Scheidt, B. Cheng, M. K. Safo, F. Cukiernik, J. C. Marchon and P. G. Debrunner, *J. Am. Chem. Soc.*, 114 (1992) 4420.
46. G. Aviles and C. K. Chang, *J. Chem. Soc., Chem. Commun.*, (1992) 31.
47. I. P. Gerothanasis, B. Loock and M. Momenteau, *J. Chem. Soc., Chem. Commun.*, (1992) 598.
48. P. Schmitt, D. Mandon, J. Fischer and R. Weiss, *New J. Chem.*, 16 (1992) 763.
49. L. Chiang, K. Konishi, T. Aida and S. Inoue, *J. Chem. Soc., Chem. Commun.*, (1992) 254.
50. J. P. Collman, X. Zhang, V. J. Lee and J. I. Brauman, *J. Chem. Soc., Chem. Commun.*, (1992) 1647.
51. H. Patzelt and W. D. Woggon, *Helv. Chim. Acta*, 75 (1992) 523.
52. W. R. Scheidt, H. Song, K. T. Hallen, M. K. Safo, R. D. Orosz, C. A. Reed and P. G. Debrunner, *Inorg. Chem.*, 31 (1992) 939.
53. K. M. Barkigia, C. K. Chang, J. Fajer and M. W. Renner, *J. Am. Chem. Soc.*, 114 (1992) 1701.

54. T. Yoshimura, H. Toi, S. Inaba and H. Ogoshi, *Bull. Chem. Soc. Jpn.*, 65 (1992) 1915.
55. A. Helms, D. Heiler and G. McLendon, *J. Am. Chem. Soc.*, 114 (1992) 6227.
56. T. G. Traylor, D. Magde, J. Luo, K. N. Walda, D. Bandyopadhyay, G. Z. Wu and V. S. Sharma, *J. Am. Chem. Soc.*, 114 (1992) 9011.
57. D. Taube, T. G. Traylor, D. Magde, K. Walda and J. Luo, *J. Am. Chem. Soc.*, 114 (1992) 9182.
57a. T. G. Traylor, J. Luo, J. A. Simon and P. C. Ford, *J. Am. Chem. Soc.*, 114 (1992) 4340.
58. T. G. Traylor, K. W. Hill, W. Fann, S. Tsuchiya and B. E. Dunlap, *J. Am. Chem. Soc.*, 114 (1992) 1308.
59. S. Ozawa, H. Fujii and I. Morishima, *J. Am. Chem. Soc.*, 114 (1992) 1548.
60. S. Ozawa, Y. Watanabe and I. Morishima, *Inorg. Chem.*, 31 (1992) 4042.
61. I. K. Choi and M. D. Ryan, *New J. Chem.*, 16 (1992) 591.
62. L. A. Andersson, M. Mylrajan, T. M. Loehr, E. P. Sullivan Jr and S. H. Strauss, *New J. Chem.*, 16 (1992) 569.
63. S. Zhang, K. S. Snyder and R. E. Shepherd, *Inorg. Chim. Acta*, 201 (1992) 223.
64. K. Linn, D. Masi, C. Mealli, C. Bianchini and M. Peruzzini, *Acta Crystallogr., Sect. C*, 48 (1992) 2220.
65. A. Cousson, F. Nectoux and E. N. Rizkalla, *Acta Crystallogr., Sect. C*, 48 (1992) 1354.
66. Y. Tor, J. Libman, A. Shanzer, C. E. Felder, S. Lifson, *J. Am. Chem. Soc.*, 114 (1992) 6661.
67. G. Xiao, D. Van der Helm, R. C. Hider and P. S. Dobbin, *J. Chem. Soc., Dalton Trans.*, (1992) 3265.
68. S. C. Shoner and P. P. Power, *Inorg. Chem.*, 31 (1992) 1001.
69. M. Leluk, B. Jezowska-Trzebiatowska and T. Lis, *Polyhedron*, 11 (1992) 1923.
70. E. Bouwman, J. C. Huffman, E. B. Lobkovsky, G. Christon, H. L. Tsai and D. N. Hendrickson, *Inorg. Chem.*, 31 (1992) 4436.
71. D. Matt, D. Lakkis, D. Grandjean, F. Balegroune and A. Laidoudi, *Acta Crystallogr., Sect. C*, 48 (1992) 1408.
72. D. L. Hughes, M. Jimenez-Tenorio, G. J. Leigh, A. Houlton and J. Silver, *J. Chem. Soc., Dalton Trans.*, (1992) 2033.
73. S. Tanaka and G. Matsubayashi, *J. Chem. Soc., Dalton Trans.*, (1992) 2837.
74. L. E. Maelia, M. Millar and S. A. Koch, *Inorg. Chem.*, 31 (1992) 4594.
75. N. Bampos, L. D. Field and T. W. Hambley, *Polyhedron*, 11 (1992) 1213.
76. D. Zirong, S. Bhattacharya, J. K. McClusker, P. M. Hagen, D. N. Hendrickson and C. G. Pierpont, *Inorg. Chem.*, 31 (1992) 870.
77. M. J. Cohn, C. Xie, J. M. Tuchagues, C. G. Pierpont and D. N. Hendrickson, *Inorg. Chem.*, 31 (1992) 5028.
78. M. Koikawa, H. Okawa, Y. Maeda and S. Kida, *Inorg. Chim. Acta*, 194 (1992) 75.
79. A. Neves, S. M. D. Erthal, V. Drago, K. Griesar and W. Haase, *Inorg. Chim. Acta*, 197 (1992) 121.
80. H. C. Tung, C. Kang and D. T. Sawyer, *J. Am. Chem. Soc.*, 114 (1992) 3445.
81. P. A. Ganeshpure, D. Kar and S. Satish, *Transition Metal Chem. (London)*, 17 (1992) 212.
82. M. Dusek, V. Petricek, J. Kamenicek and Z. Sindelar, *Acta Crystallogr., Sect. C*, 48 (1992) 1579.
83. A. W. Schwabacher, J. Lee and H. Lei, *J. Am. Chem. Soc.*, 114 (1992) 7597.
84. M. Akiyama, A. Katoh, M. Iijima, T. Takagi, K. Natori and T. Kojima, *Bull. Chem. Soc. Jpn.*, 65 (1992) 1356.
85. Y. Maeda, Y. Noda, H. Oshio, Y. Takashima, *Bull. Chem. Soc. Jpn.*, 65 (1992) 1825.
86. M. T. S. Amorim, R. Delgado and J. J. R. Frausto da Silva, *Polyhedron*, 11 (1992) 1891.
87. C. Flassbeck and K. Wieghardt, *Z. Anorg. Allg. Chem.*, 608 (1992) 60.
88. K. Ramesh and R. Mukherjee, *J. Chem. Soc., Dalton Trans.*, (1992) 83.
89. X. Wang, W. T. Pennington, D. L. Ankers, J. C. Fanning, *Polyhedron*, 11 (1992) 2253.
90. A. Schaefer, B. Fischer, H. Paul, R. Bossahard, M. Hesse and M. Viscontini, *Helv. Chim. Acta*, 75 (1992) 1955.
91. M. E. Bodini, C. Estefo M. and M. A. Del Valle, *Polyhedron*, 11 (1992) 2203.
92. J. Real, B. Gallois, T. Granier, F. Suez-Panama and J. Zaembowitch, *Inorg. Chem.*, 31 (1992) 4972.
93. A. El-Shekeil and A. Z. El-Sonbati, *Transition Metal Chem. (London)*, 17 (1992) 420.
94. J. P. Scovill, M. W. Blaney, D. X. West, A. E. Liberta and L. K. Pannell, *Transition Metal Chem. (London)*, 17 (1992) 377.
95. H. Singh, V. K. Srivastava, S. N. Shukla and M. K. Upadhyaya, *Indian J. Chem. Sect. A*, 31 (1992) 472.

96. D. Sellman, W. Soglowek, F. Knock, G. Ritter and J. Dengler, *Inorg. Chem.*, 31 (1992) 3711.
97. K. Abu-Dari and K. N. Raymond, *J. Coord. Chem.*, 26 (1992) 1.
98. R. B. Lanjewar and A. N. Garg, *Indian J. Chem., Sect. A:, 31* (1992) 849.
99. U. Jayasooriya, R. D. Cannon and C. E. Anson, *J. Chem. Soc., Chem. Commun.*, (1992) 379.
100. V. A. Vankai, M. G. Newton and D. M. Kurtz, Jr., *Inorg. Chem.*, 31 (1992) 341.
101. N. Kitajima, N. Tamura, M. Tanaka, Y. Moro-Oka, *Inorg. Chem.*, 31 (1992) 3342 .
102. R. L. Rardin, P. Poganiuch, A. Bino, D. P. Goldberg, W. B. Tolman, S. Liu and S. J. Lippard, *J. Am. Chem. Soc.*, 114 (1992) 5240.
103. A. A. Shteinmann, *Mendeleev Commun.*, (1992), 155.
104. K. L. Taft, A. Masschelein, S. Liu and S. J. Lippard, *Inorg. Chim. Acta*, 198 (1992) 627.
105. M. S. Mashuta, R. J. Webb, J. K. McClusker, E. A. Schmitt, K. J. Oberhausen, J. F. Richardson, R. M Buchanan and D. N. Hendrickson, *J. Am. Chem. Soc.*, 114 (1992) 3815.
106. S. Menage, Y. Zang, M. P. Hendrich and L. Que, Jr., *J. Am. Chem. Soc.*, 114 (1992) 7786.
107. J. R. Hart, A. K. Rappé, S. M. Gorun and T. H. Upton, *Inorg. Chem.*, 31 (1992) 5254.
108. S. L. Heath, A. K. Powell, H. L. Utting and M. Helliwell, *J. Chem. Soc., Dalton Trans.*, (1992) 305.
109. K. S. Hagen and R. Lachiotte, *J. Am. Chem. Soc.*, 114 (1992) 8741.
110. J. K. Oberhauser, J. F. Richardson, R. J. O'Brien, R. M. Buchanan, J. K. McClusker, R. J. Webb and D. N. Henrickson, *Inorg. Chem.*, 31 (1992) 1123.
111. Y. Nishida, M. Nasu and T. Akamatsu, *Z. Naturforsch., B*, 47 (1992) 115.
112. Y. Nishida, M. Nasu and T. Akamatsu, *J. Chem. Soc., Chem. Commun.*, (1992) 93.
113. A. M. Khenkin and M. L. Stepanova, *Mendeleev Commun.*, (1992) 57.
114. S. Mahapatra, N. Gupta and R. Mukherjee, *J. Chem. Soc., Dalton Trans.*, (1992) 3041.
115. R. Hotzelmann, K. Weighardt, J. Ensling, H. Romstedt, P. Guetlich, E. Bill, U. Floerke and H. J. Haupt, *J. Am. Chem. Soc.*, 114 (1992) 9470.
116. R. Hotzelmann, K. Wieghardt, U. Floerke, H. J. Haupt, D. C. Weatherburn, J. Bonvosin, G. Blondin and J. J. Girerd, *J. Am. Chem. Soc.*, 114 (1992) 1681.
117. L. D. Schultz, G. D. Fallon, B. Moubaraki, K. S. Murray, B. O. West, *J. Chem. Soc., Chem. Commun.*, (1992) 971.
118. K. Hegetschweiler, H. W. Schmalle, H. M. Streit, V. Gramlich, H. U. Hund, I. Erni, *Inorg. Chem.*, 31 (1992) 1299.
119. V. S. Nair and K. S. Hagen, *Inorg. Chem.*, 31 (1992) 4048.
120. S. L. Heath, A. K. Powell, *Angew. Chem., Int. Ed. Engl.*, 31 (1992) 191.
121. H. L. Blonk, J. Mesmen, J. G. M. Van der LInden, J. J. Steggerda, J. M. M. Smits, P. T. Beurskens, C. Tonon and J. Jordanov, *Inorg. Chem.*, 31 (1992) 963.
122. E. K. H. Roth and J. Jordanov, *Inorg. Chem.*, 31 (1992) 240.
123. S. Inomata, H. Tobita and H. Ogino, *Inorg. Chem.*, 31 (1992) 722.
124. D. J. Evans, G. Garcia, G. J. Leigh, M. S. Newton, M. D. Santana, *J. Chem. Soc., Dalton Trans.*, (1992) 3229.
125. C. N. Chau and A. Wojcicki, *Polyhedron*, 11 (1992) 851.
126. C. Glidewell and R. J. W. Lambert, *Polyhedron*, 11 (1992) 2803.
127. F. Cecconi, C. A. Ghilardi, S. Midollini and A. Orlandini, *J. Chem. Soc., Chem. Commun.*, (1992) 910.
128. A. R. Butler, C. Glidewell and S. M. Glidewell, *J. Chem. Soc., Chem Commun.*, (1992) 141.
129. A. R. Butler, C. Glidewell and S. M. Glidewell, *Polyhedron*, 11 (1992) 591.
130. D. Coucouvanis, S. A. Al-Ahmad, A. Salifoglou, V. Papaefthymoiu, A. Kostikas and A. Simpoulos, *J. Am. Chem. Soc.*, 114 (1992) 2472.
131. S. Ciurli, P. K. Ross, M. J. Scott, S. B. Yu and R. H. Holm, *J. Am. Chem. Soc.*, 114 (1992) 5415.
132. J. Zhou, M. J. Scott, Z. Hu, G. Peng, E. Munck and R. H. Holm, *J. Am. Chem. Soc.*, 114 (1992) 10843.
133. J. F. You, G. C. Papaefthymiou and R. H. Holm, *J. Am. Chem. Soc.*, 114 (1992) 2697.